

SUPPORTING INFORMATION

Polyethylenimine-Bisphosphonate-Cyclodextrin Ternary Conjugates: Supramolecular Systems for the Delivery of Antineoplastic Drugs

Simona Plesselova,^{a,d,†} Pablo Garcia-Cerezo,^{b,d,†} Víctor Blanco,^{b,d} Francisco J. Reche-Perez,^{a,d} Fernando Hernandez-Mateo,^{b,c,d} Francisco Santoyo-Gonzalez,^{b,c,d*} María Dolores Giron-Gonzalez,^{a,d} and Rafael Salto-Gonzalez^{a,d*}

^aDepartment of Biochemistry and Molecular Biology II, School of Pharmacy, University of Granada, E-18071 Granada, Spain

^bDepartment of Organic Chemistry, School of Sciences, University of Granada, E-18071 Granada, Spain

^cBiotechnology Institute, University of Granada, E-18071 Granada, Spain

^dUnit of Excellence in Chemistry Applied to Biomedicine and the Environment of the University of Granada, E-18071 Granada, Spain

Corresponding Authors e-mails: rsalto@ugr.es; fsantoyo@ugr.es

List of Contents

1. Synthesis and characterization of PEI-BP-CD (20-21a,b) and PEI-MP-CD (22a,b) ternary systems	S3
2. NMR Spectra	S4
3. HRMS Spectra of key Products	S35
5. Particle size of the PEI-BP-CD ternary conjugates	S42
6. Subcellular fractionation of MG-63 cells	S43
7. Effects of inhibitors of internalization routes on DOX_{21b} uptake	S44
8. Specific PEI-BP-CD (20-21b) and PEI-MP-CD (22b) conjugates uptake in bone cells	S45
9. <i>In vivo</i> imaging of tumor MDA-MB-231 xenografts in mice	S46

1. Synthesis of PEI-BP-CD (20-21a,b) and PEI-MP-CD (22a,b) ternary systems

Table S1. Individual Conditions.

Entry	2kPEI (μmol)	Phosphonate (μmol)	β -CD-VS (μmol)	Compound(mg)
1	12.5	7 (12.5)	50.0	20a (95)
2	12.5	7 (25.0)	50.0	20b (47)
3	12.5	11 (12.5)	50.0	21a (76)
4	12.5	11 (25.0)	50.0	21b (82)
5	7.5	17 (7.5)	30.0	22a (54)
6	7.5	17 (15.0)	30.0	22b (57)

Compound 20a. White foam. ^{31}P NMR (202 MHz, $\text{D}_2\text{O}/\text{DMSO-d}_6$): $\delta=17.73$. IR (neat): $\nu=2969, 1740, 1367, 1216, 1026\text{ cm}^{-1}$.

Compound 20b. White foam. ^{31}P NMR (162 MHz, $\text{D}_2\text{O}/\text{DMSO-d}_6$): $\delta=17.75$. IR (neat): $\nu=2932, 1740, 1367, 1216, 1026\text{ cm}^{-1}$.

Compound 21a. White solid. ^{31}P NMR (202 MHz, $\text{D}_2\text{O}/\text{DMSO-d}_6$): $\delta=6.50$. IR (neat): $\nu=3282, 2930, 1285, 1079, 1022\text{ cm}^{-1}$.

Compound 21b. White solid. ^{31}P NMR (202 MHz, $\text{D}_2\text{O}/\text{DMSO-d}_6$): $\delta=6.89$. IR (neat): $\nu=3282, 2930, 1739, 1367, 1079, 1026\text{ cm}^{-1}$.

Compound 22a. Light yellow solid. ^{31}P NMR (202 MHz, $\text{D}_2\text{O}/\text{DMSO-d}_6$): $\delta=11.50$. IR (neat): $\nu=3271, 2923, 1738, 1365, 1078, 1024\text{ cm}^{-1}$.

Compound 22b. Light yellow solid. ^{31}P NMR (202 MHz, $\text{D}_2\text{O}/\text{DMSO-d}_6$): $\delta=11.01$. IR (neat): $\nu=2914, 1740, 1367, 1080, 1029\text{ cm}^{-1}$.

3. NMR spectra

Compound 2:

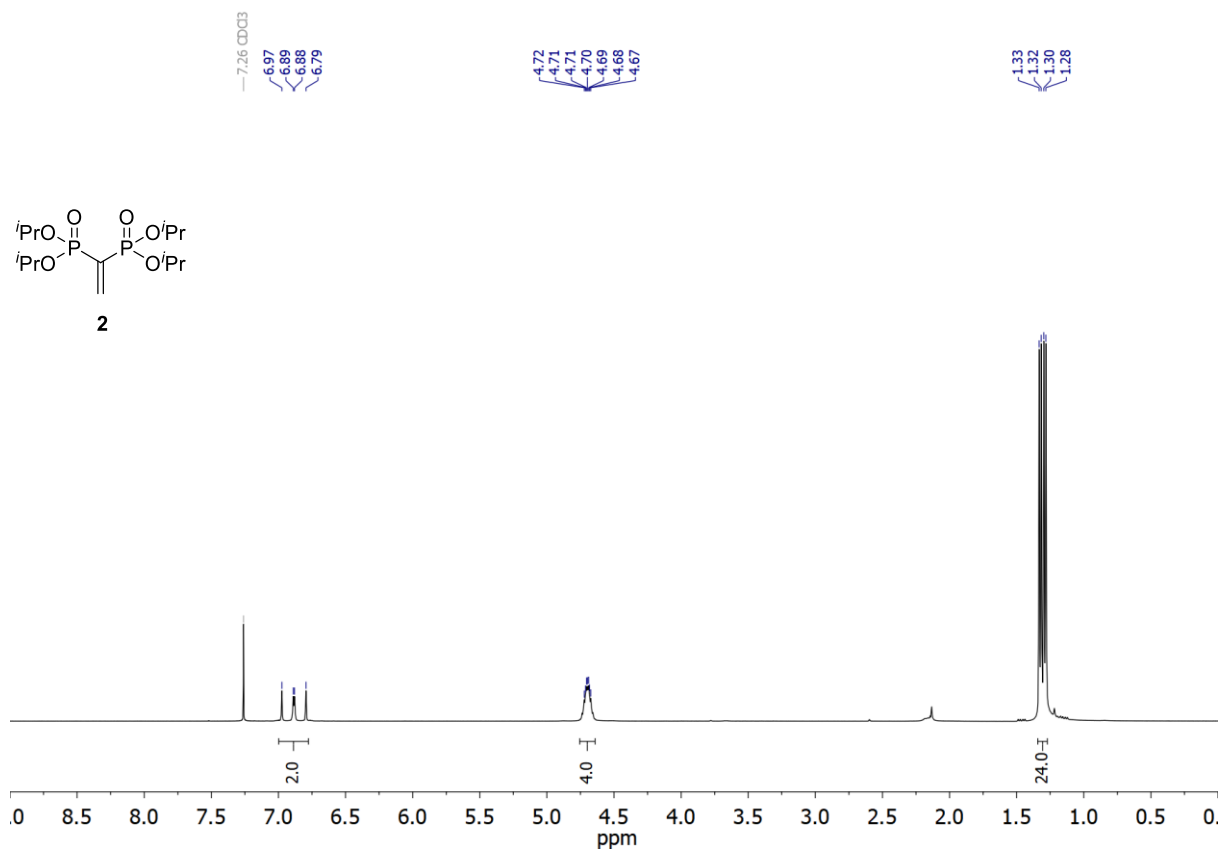


Figure S1. ¹H NMR (400 MHz, CDCl₃) spectrum of 2.

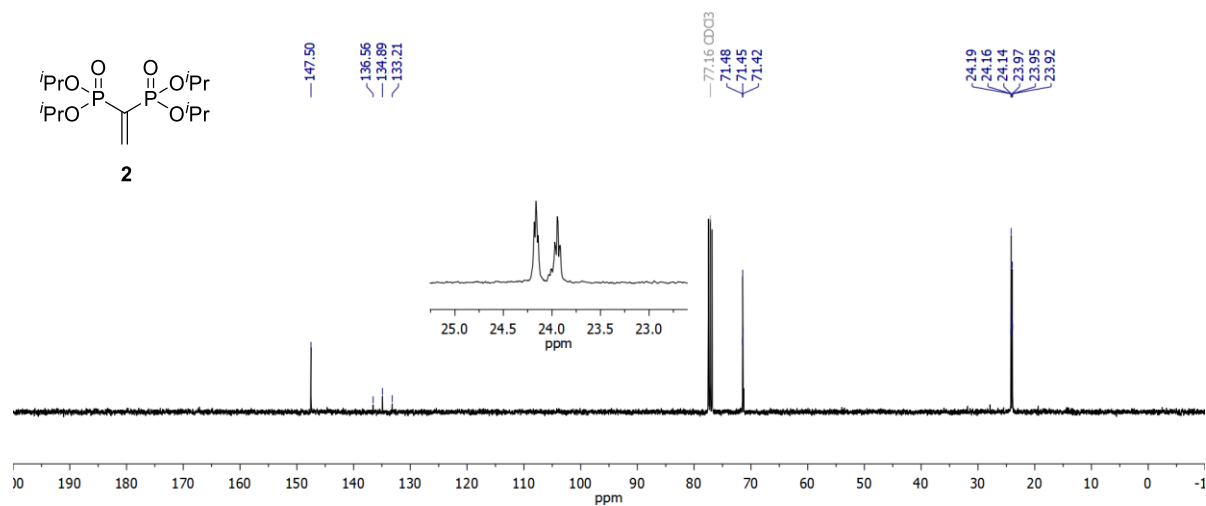


Figure S2. ¹³C NMR (101 MHz, CDCl₃) spectrum of 2.

Compound 4:

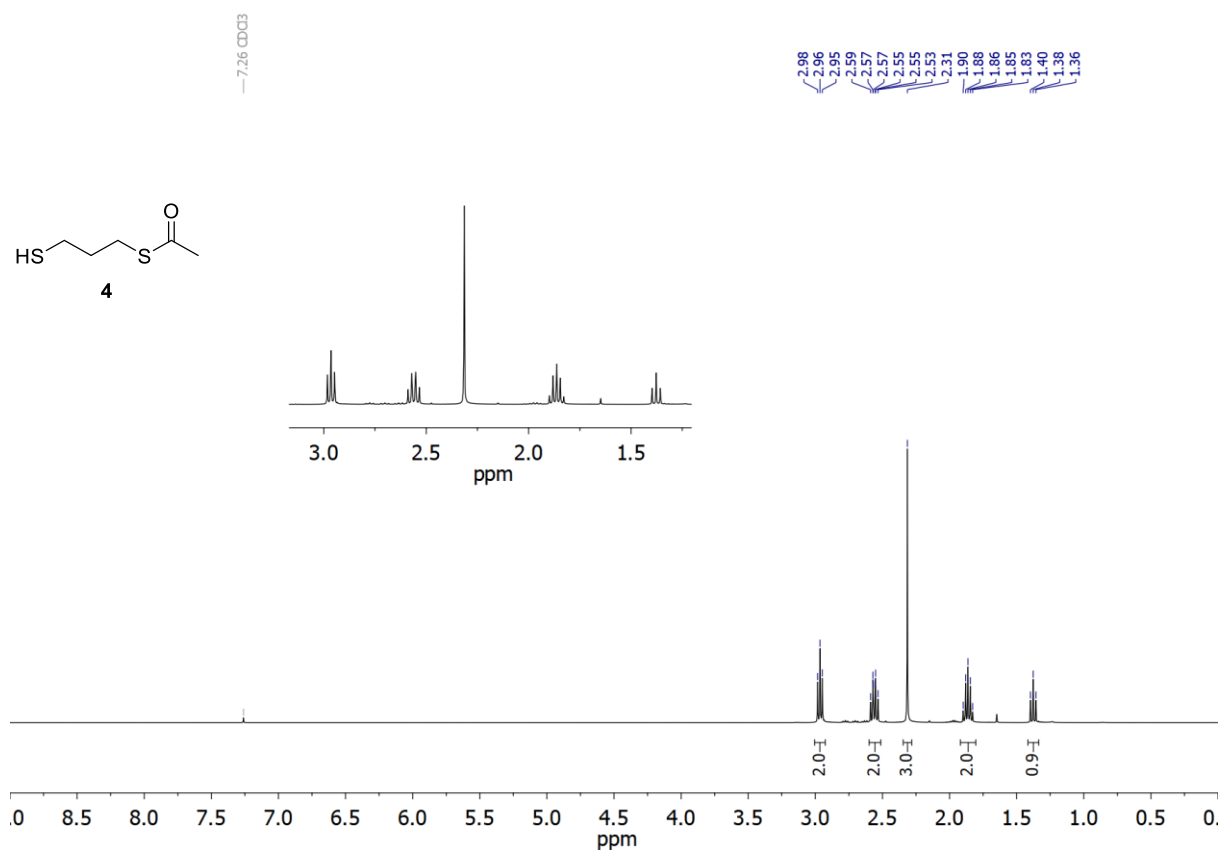


Figure S3. ¹H NMR (400 MHz, CDCl₃) spectrum of 4.

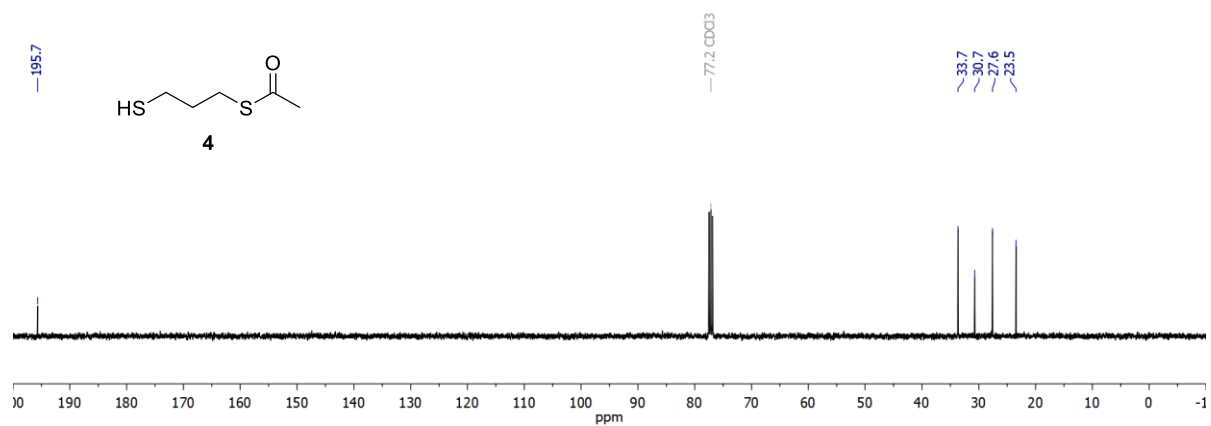
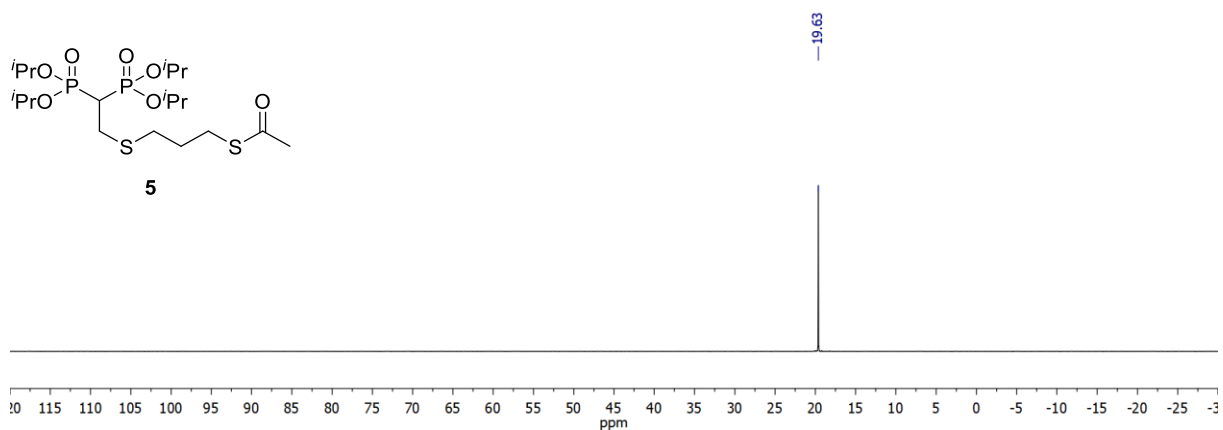
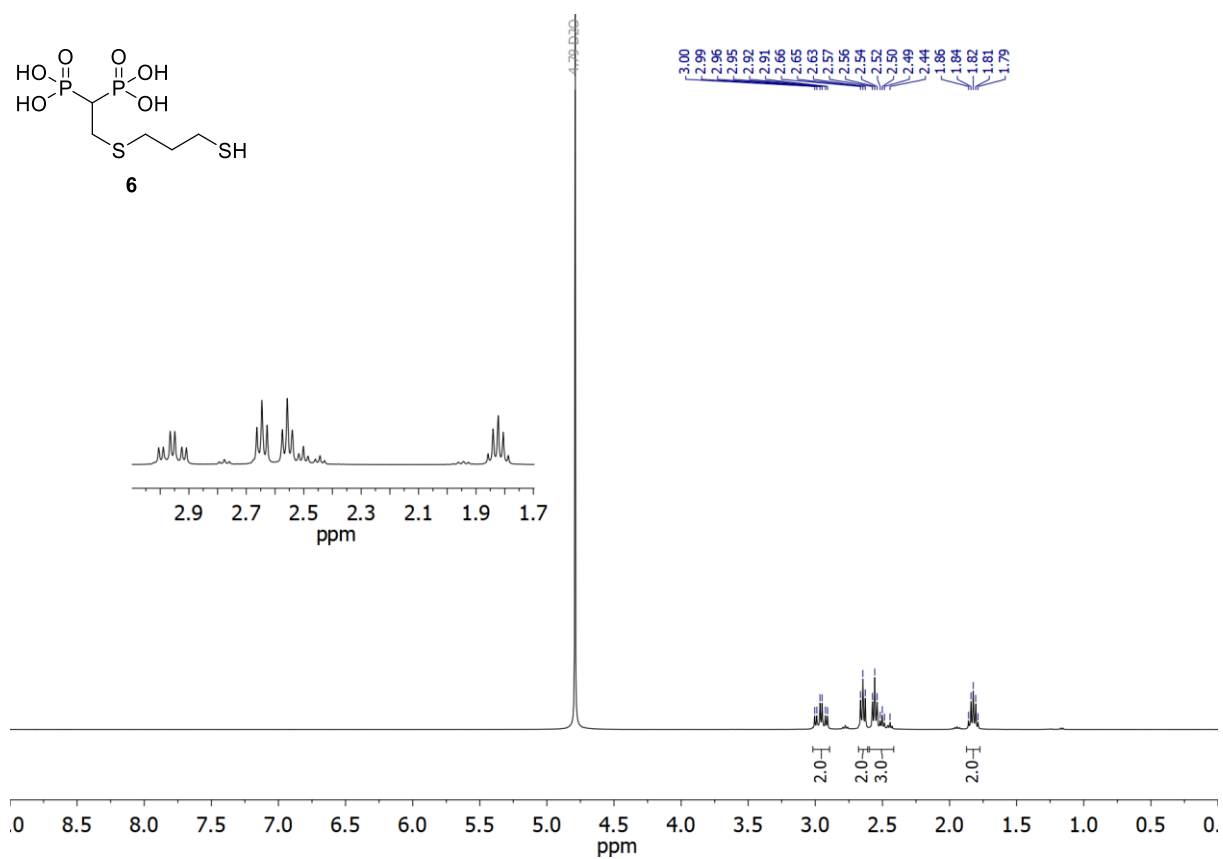


Figure S4. ¹³C NMR (101 MHz, CDCl₃) spectrum of 4.



Compound 6:



Compound 7:

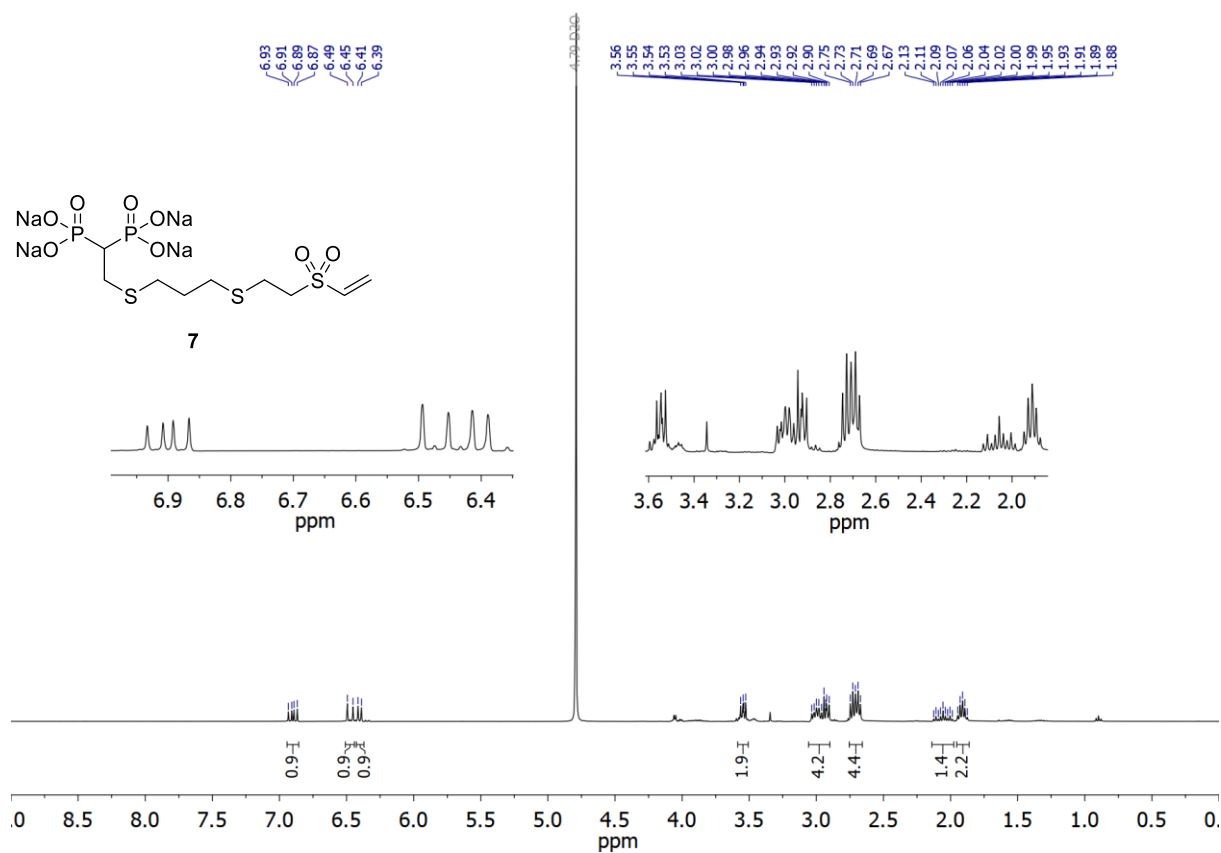


Figure S9. ¹H NMR (400 MHz, D₂O) spectrum of **7**.

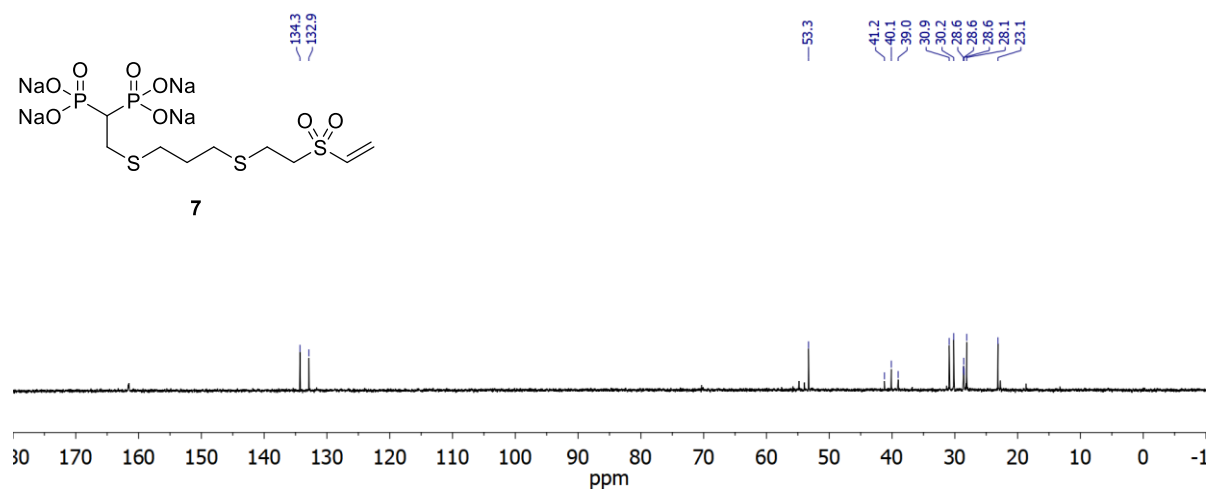


Figure S10. ¹³C NMR (101 MHz, D₂O) spectrum of **7**.

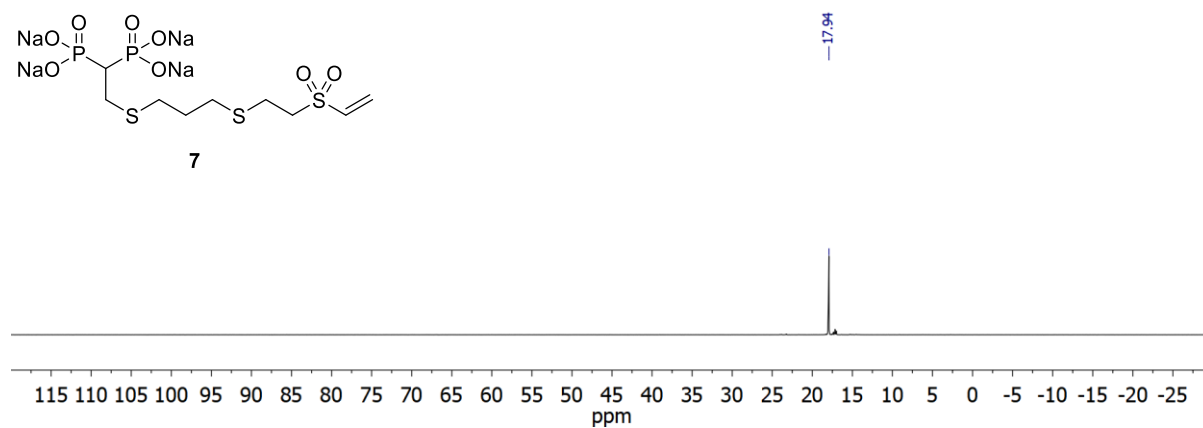
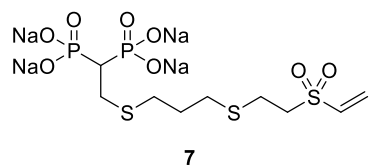


Figure S11. ^{31}P NMR (162 MHz, D_2O) spectrum of 7.

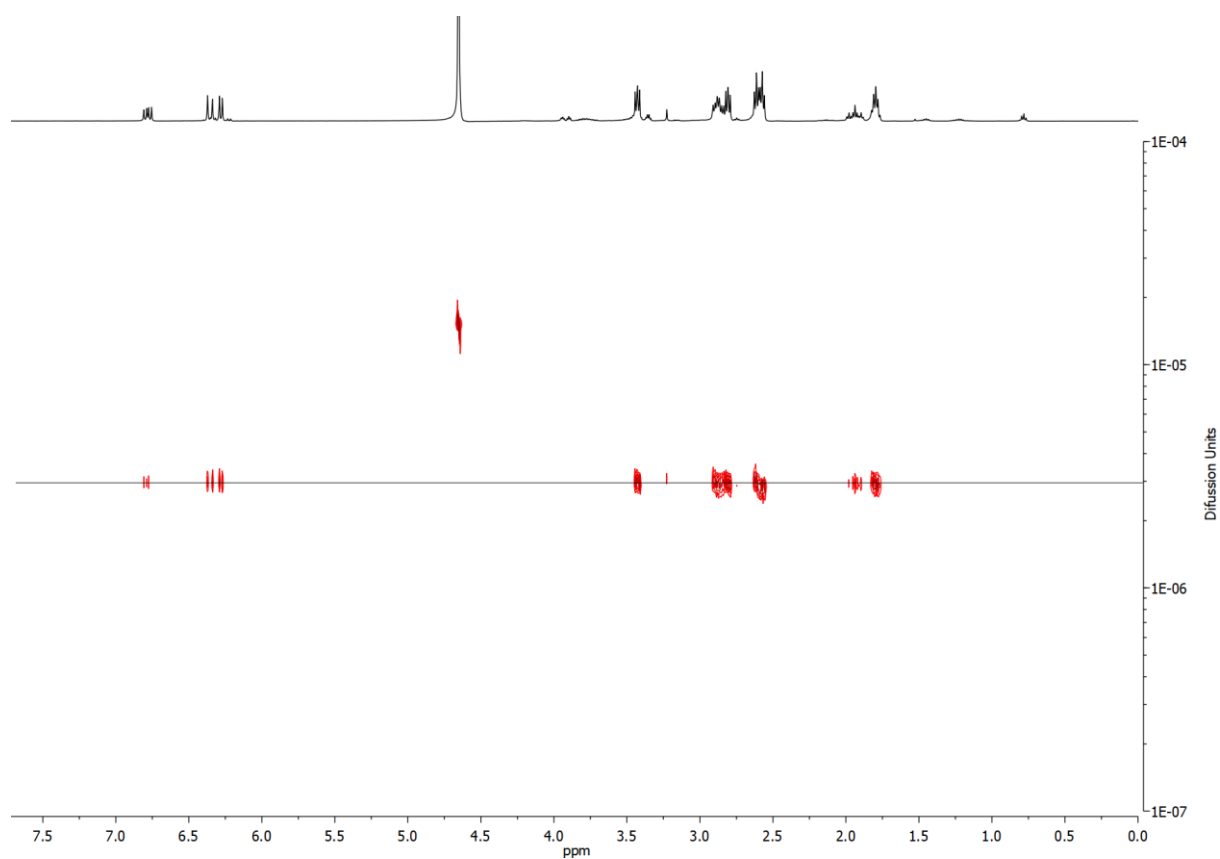


Figure S12. DOSY NMR (500 MHz, D_2O) spectrum of 7.

Compound 9:

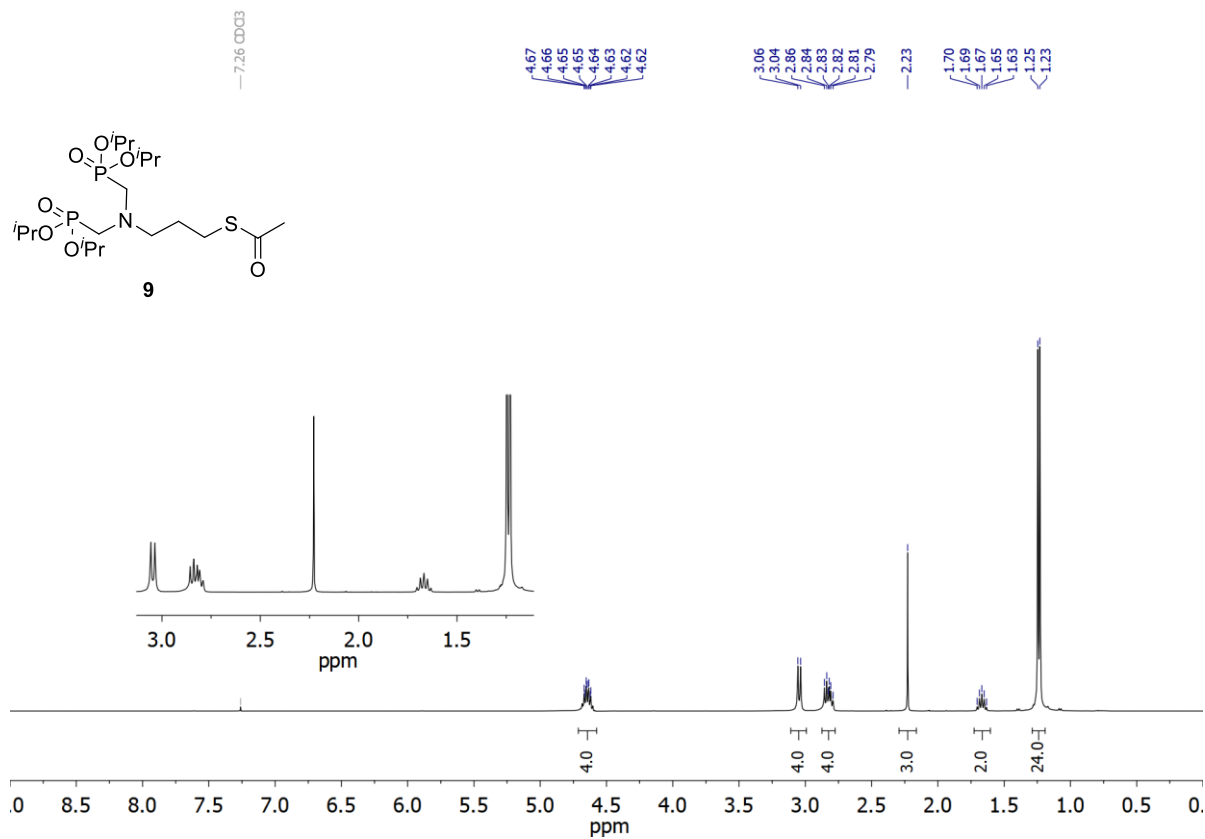


Figure S13. ¹H NMR (400 MHz, CDCl₃) spectrum of 9.

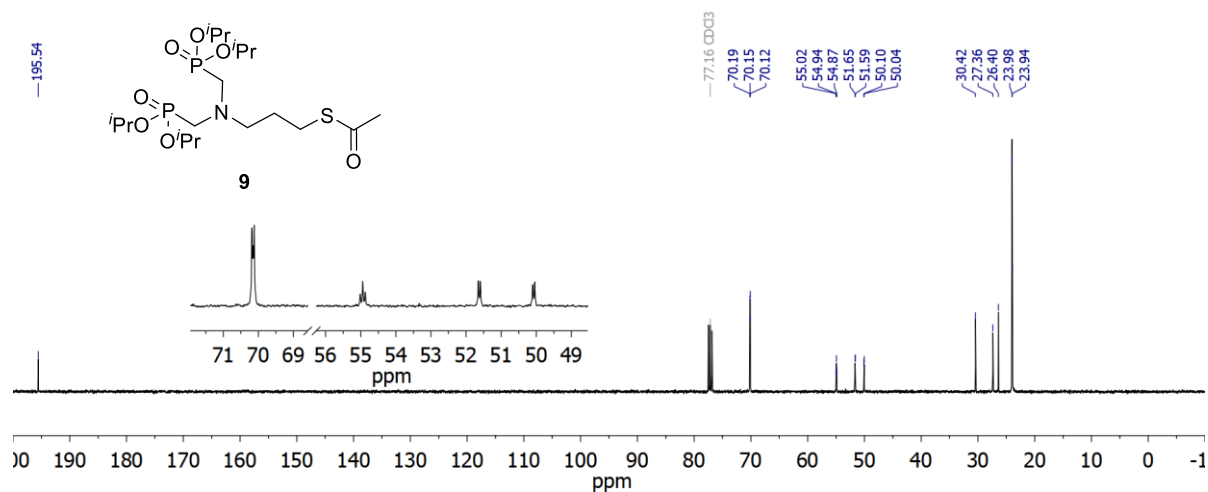


Figure S14. ¹³C NMR (101 MHz, CDCl₃) spectrum of 9.

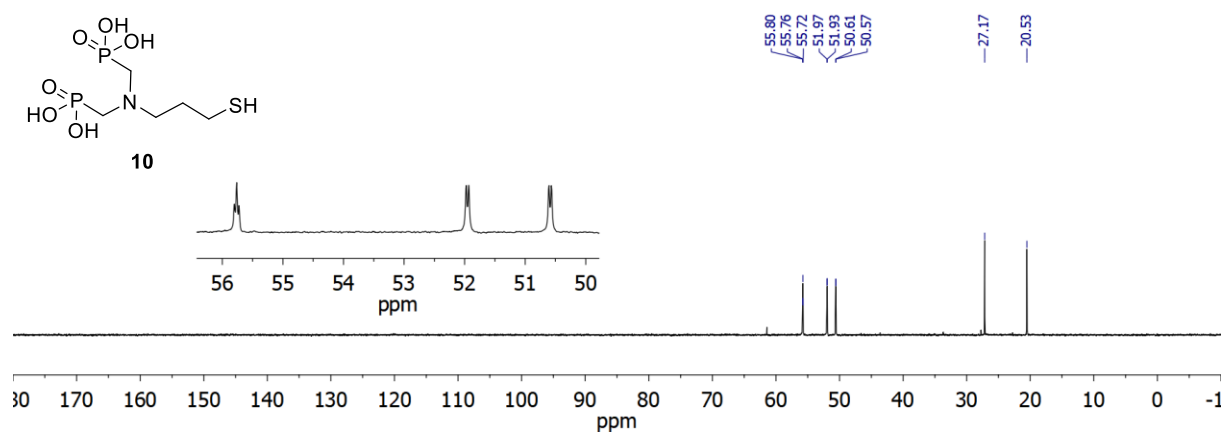


Figure S17. ^{13}C NMR (101 MHz, D_2O) spectrum of **10**.

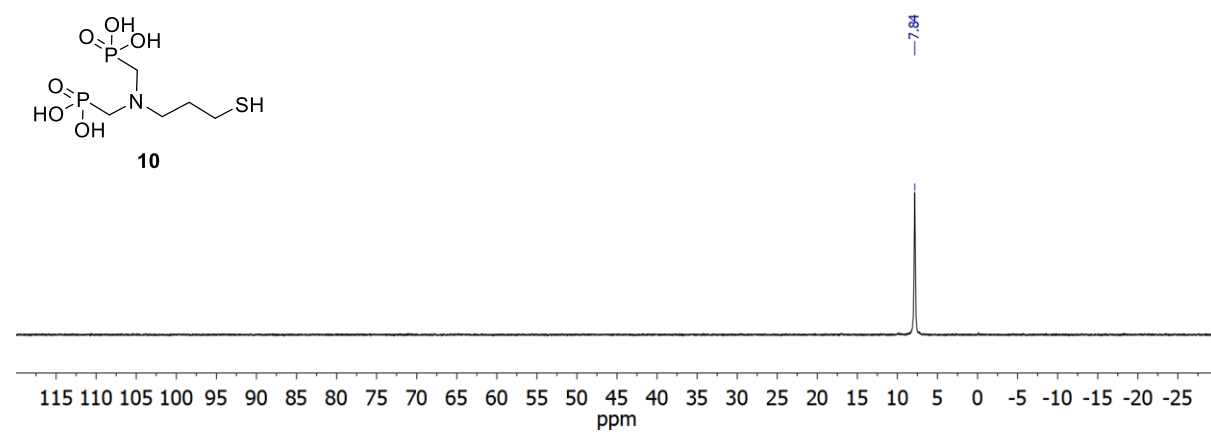


Figure S18. ^{31}P NMR (162 MHz, D_2O) spectrum of **10**.

Compound 11:

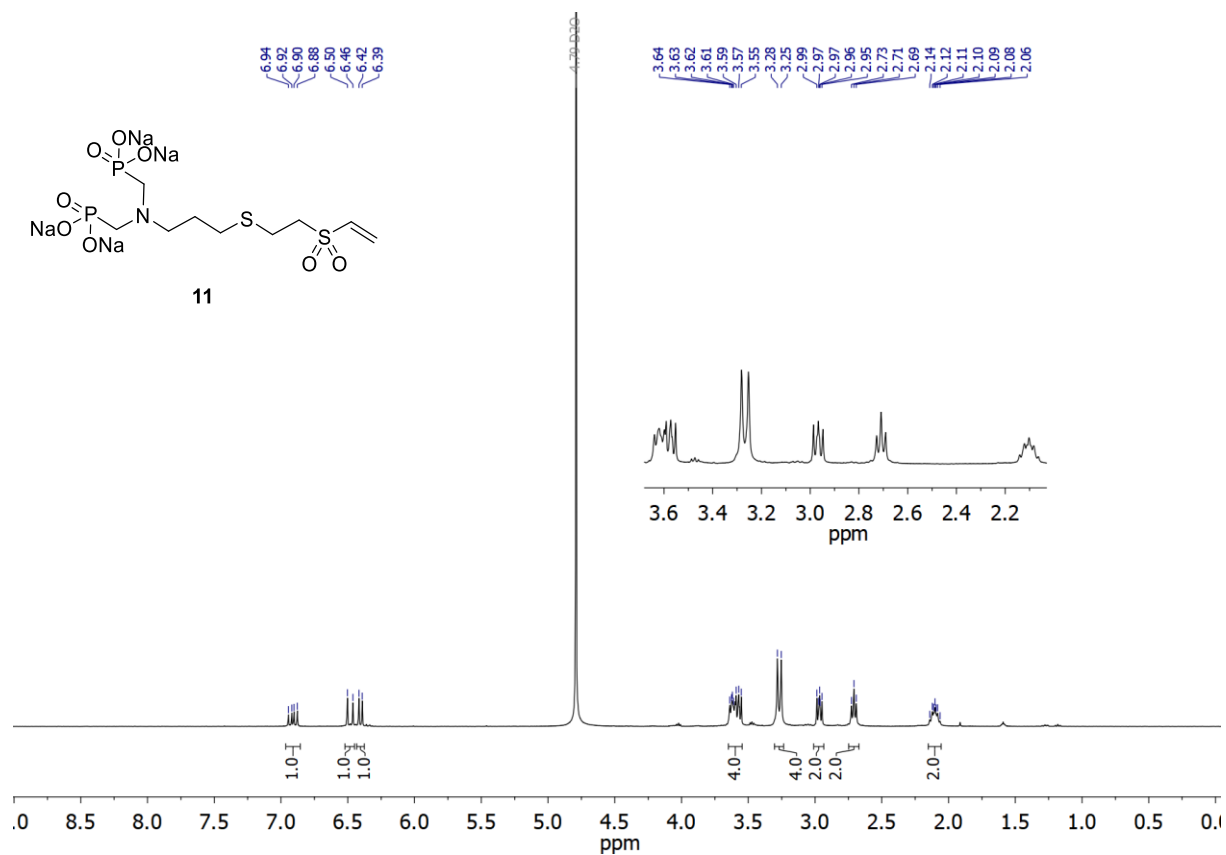


Figure S19. ¹H NMR (400 MHz, D₂O) spectrum of **11**.

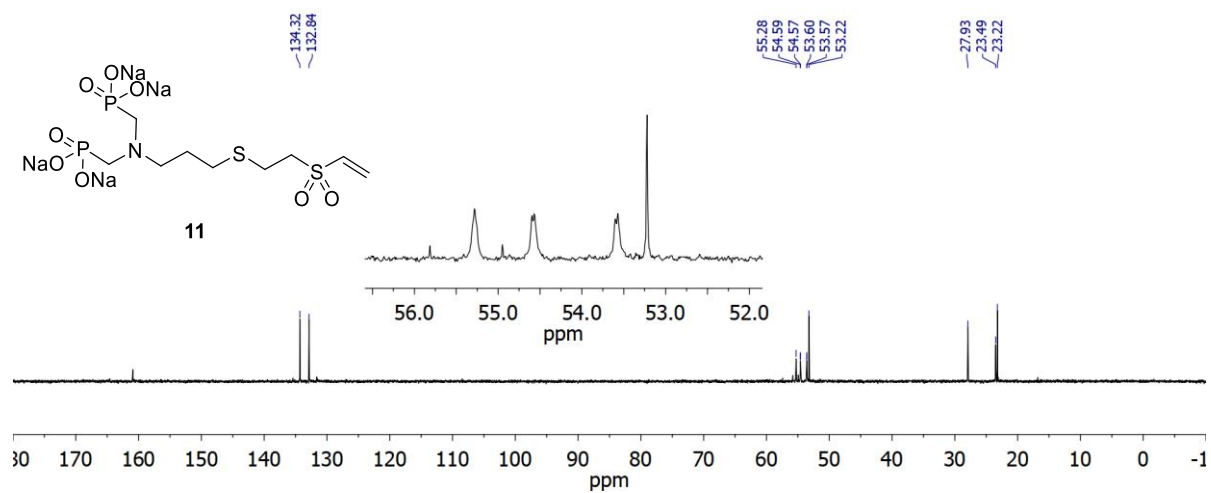


Figure S20. ¹³C NMR (126 MHz, D₂O) spectrum of **11**.

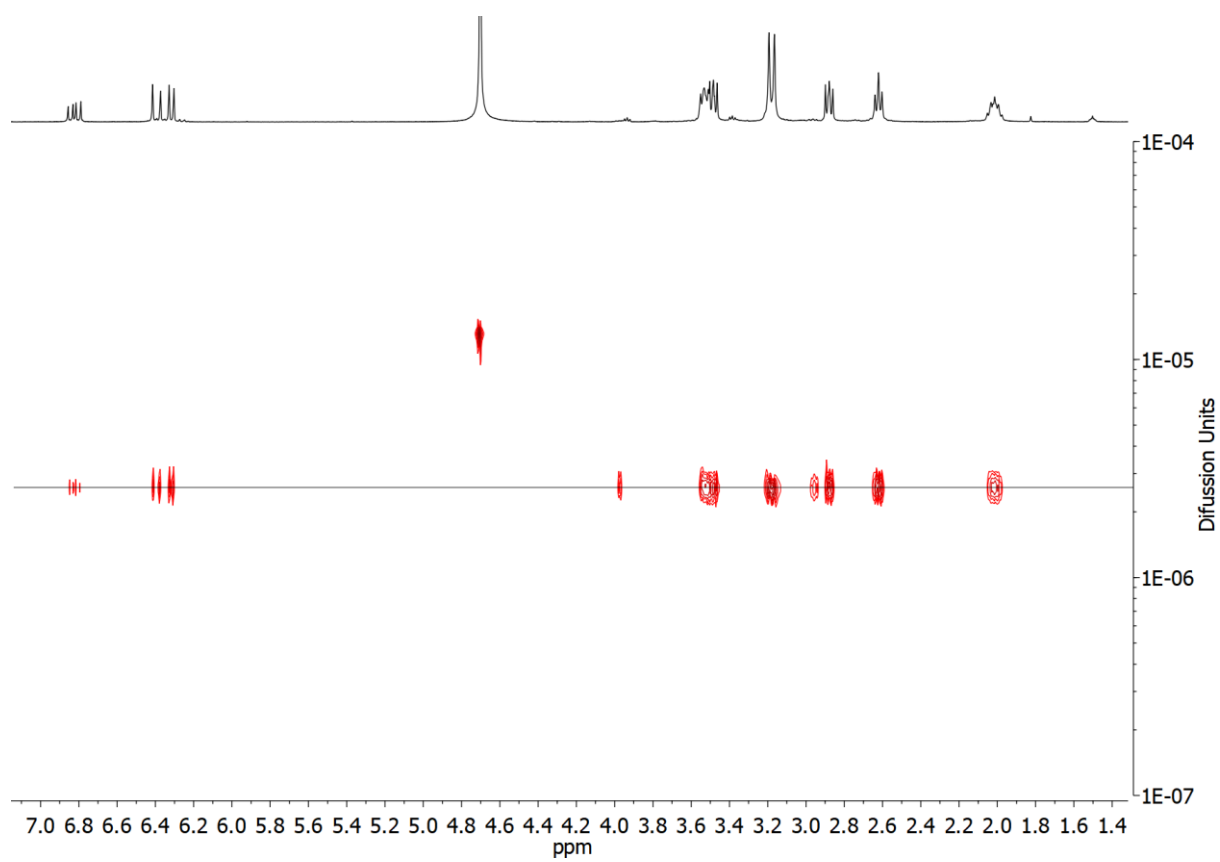
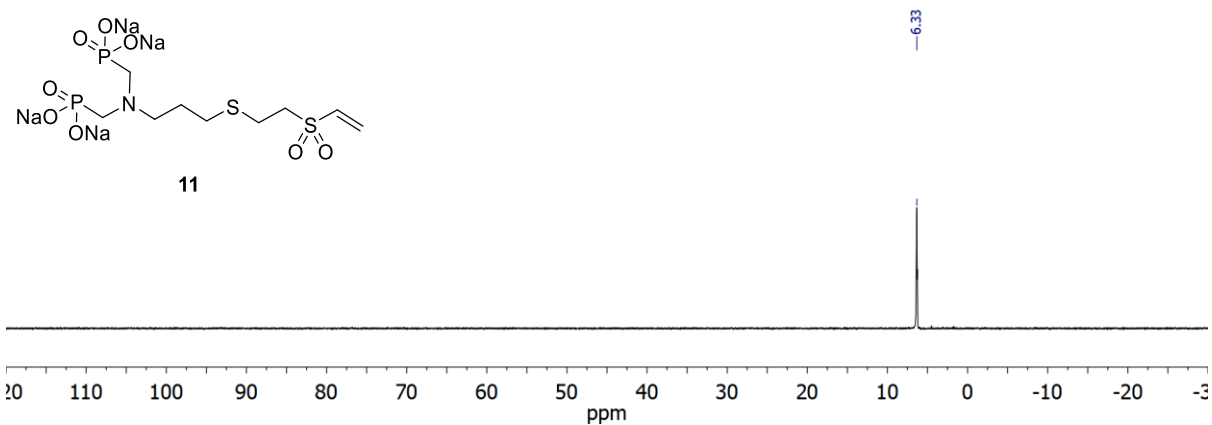


Figure S22. DOSY NMR (500 MHz, D_2O) spectrum of **11**.

Compound 13:

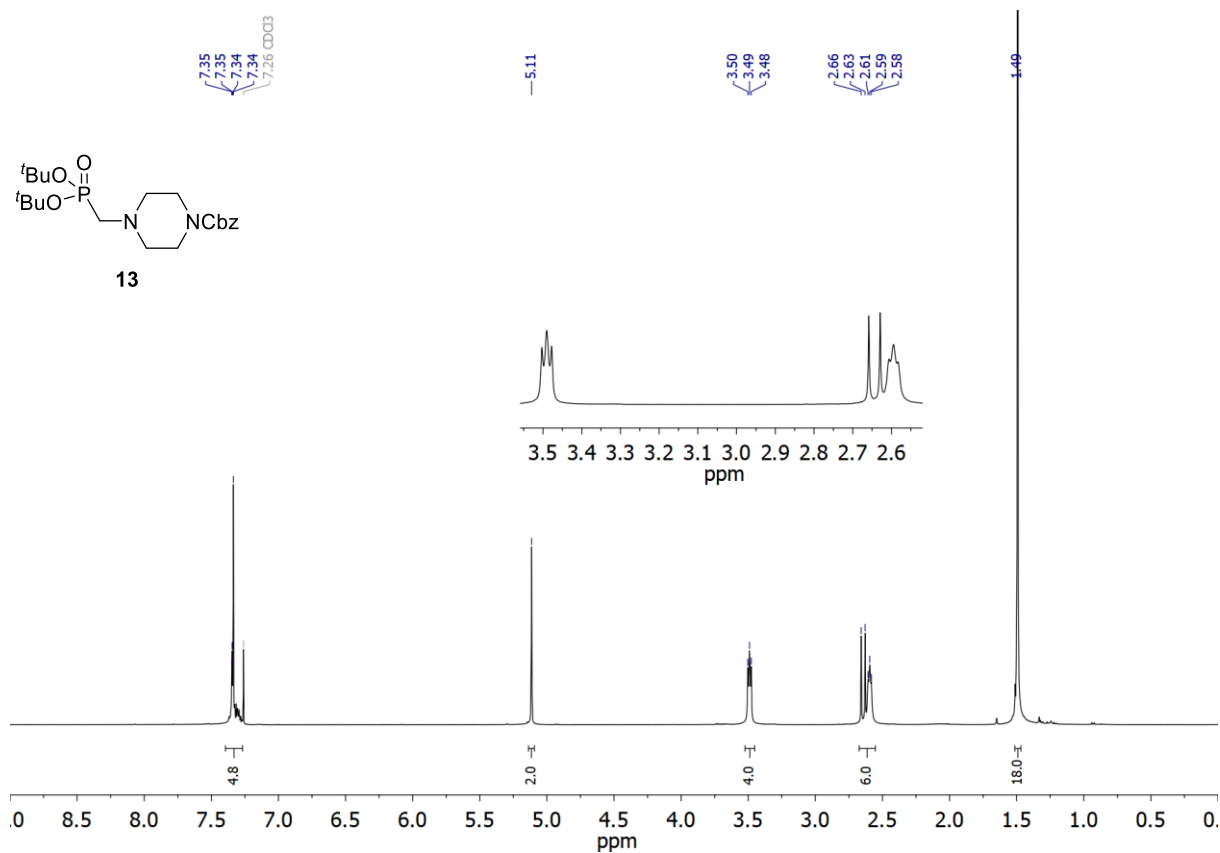


Figure S23. ¹H NMR (400 MHz, CDCl₃) spectrum of **13**.

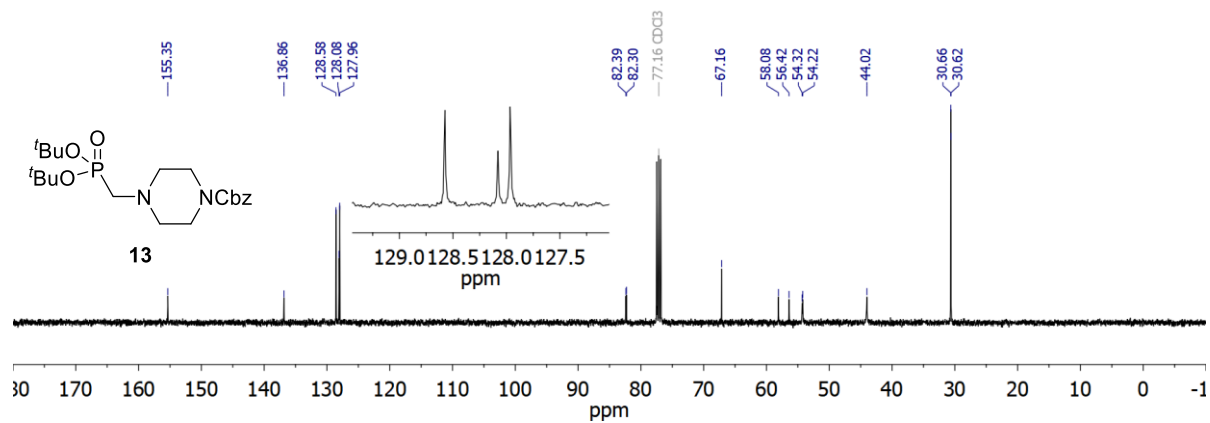
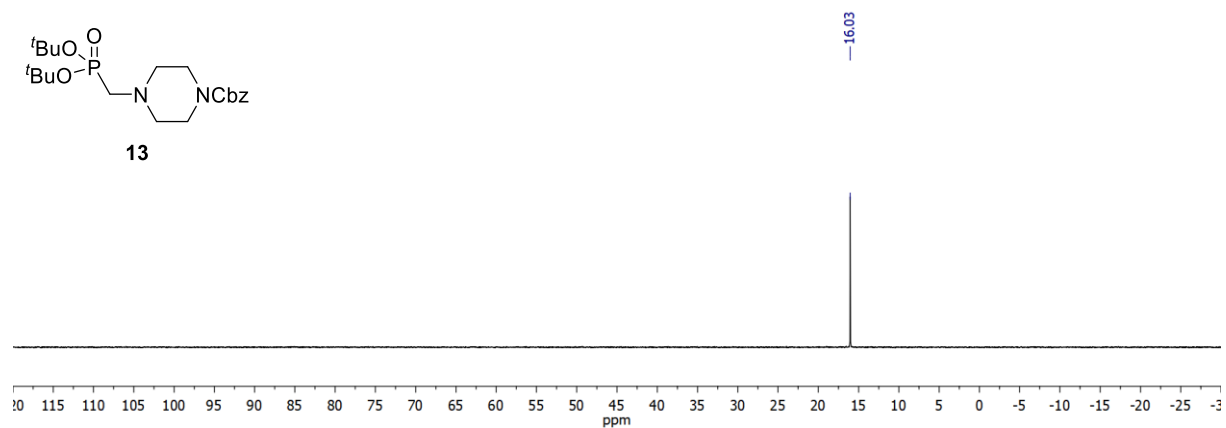
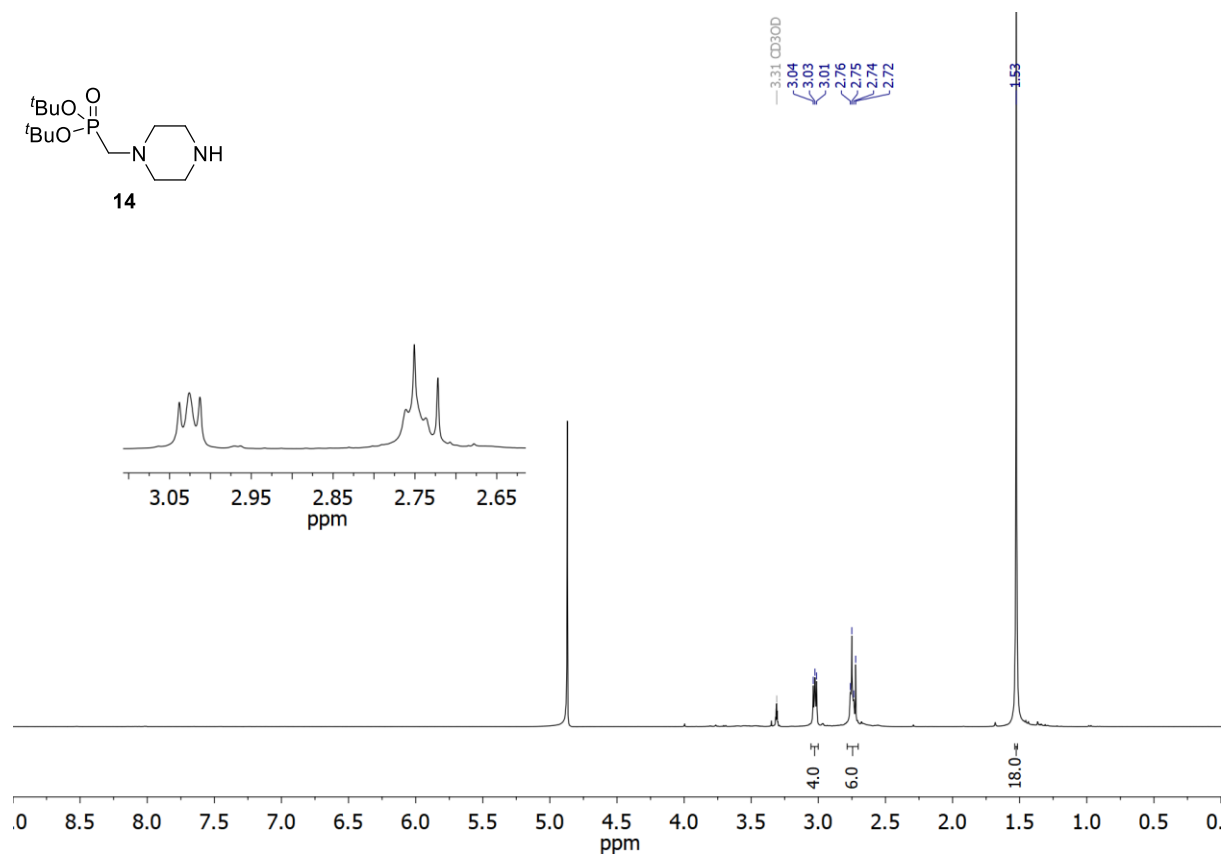


Figure S24. ¹³C NMR (101 MHz, CDCl₃) spectrum of **13**.



Compound 14:



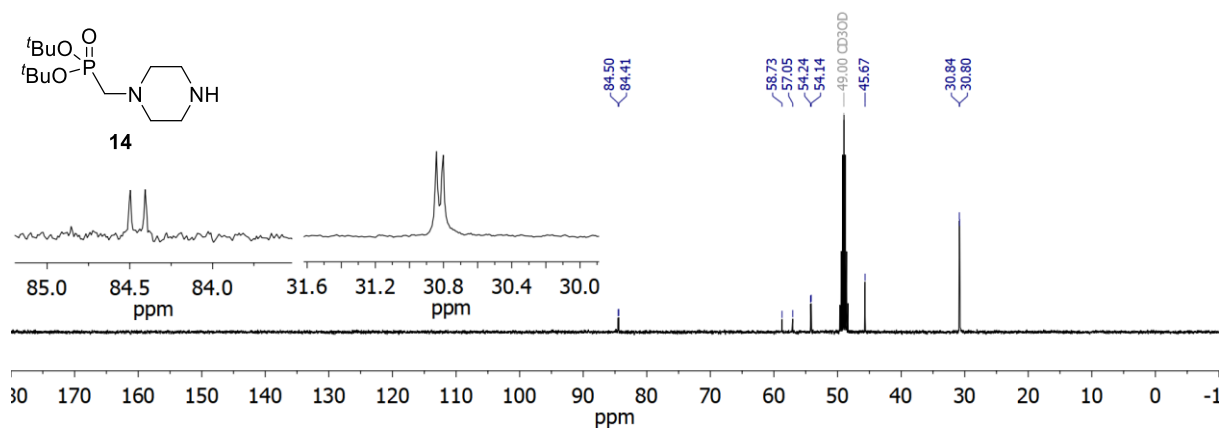


Figure S27. ^{13}C NMR (101 MHz, CD_3OD) spectrum of **14**.

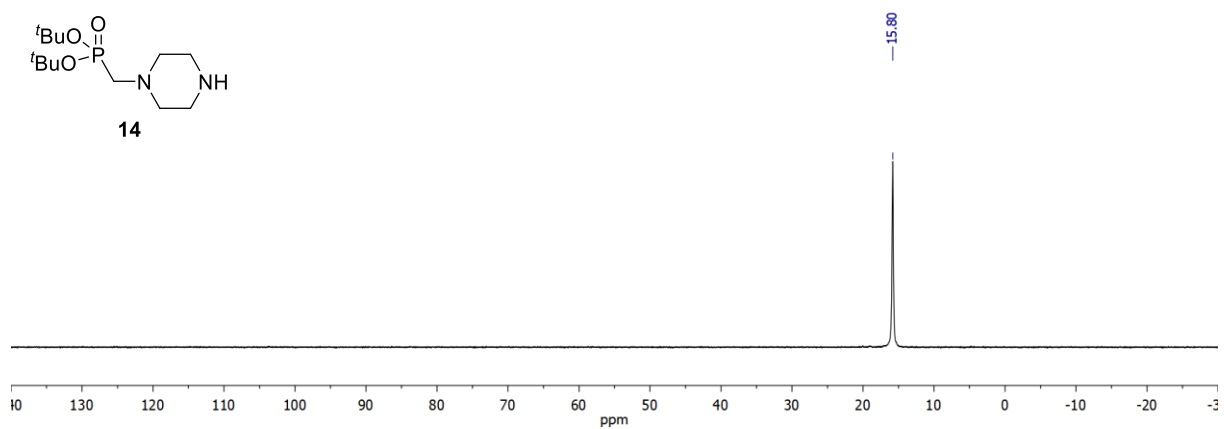


Figure S28. ^{31}P NMR (162 MHz, CD_3OD) spectrum of **14**.

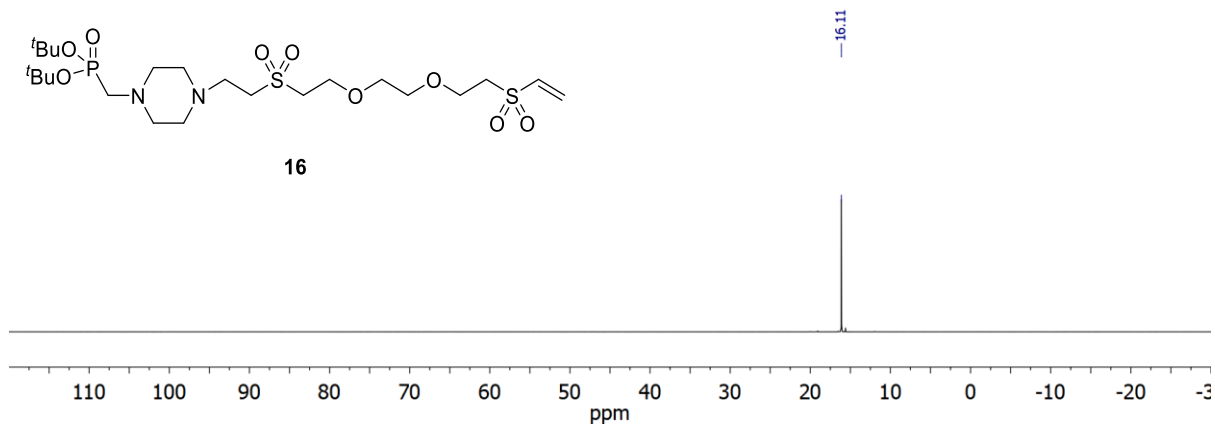


Figure S31. ^{31}P NMR (202 MHz, CDCl_3) spectrum of **16**.

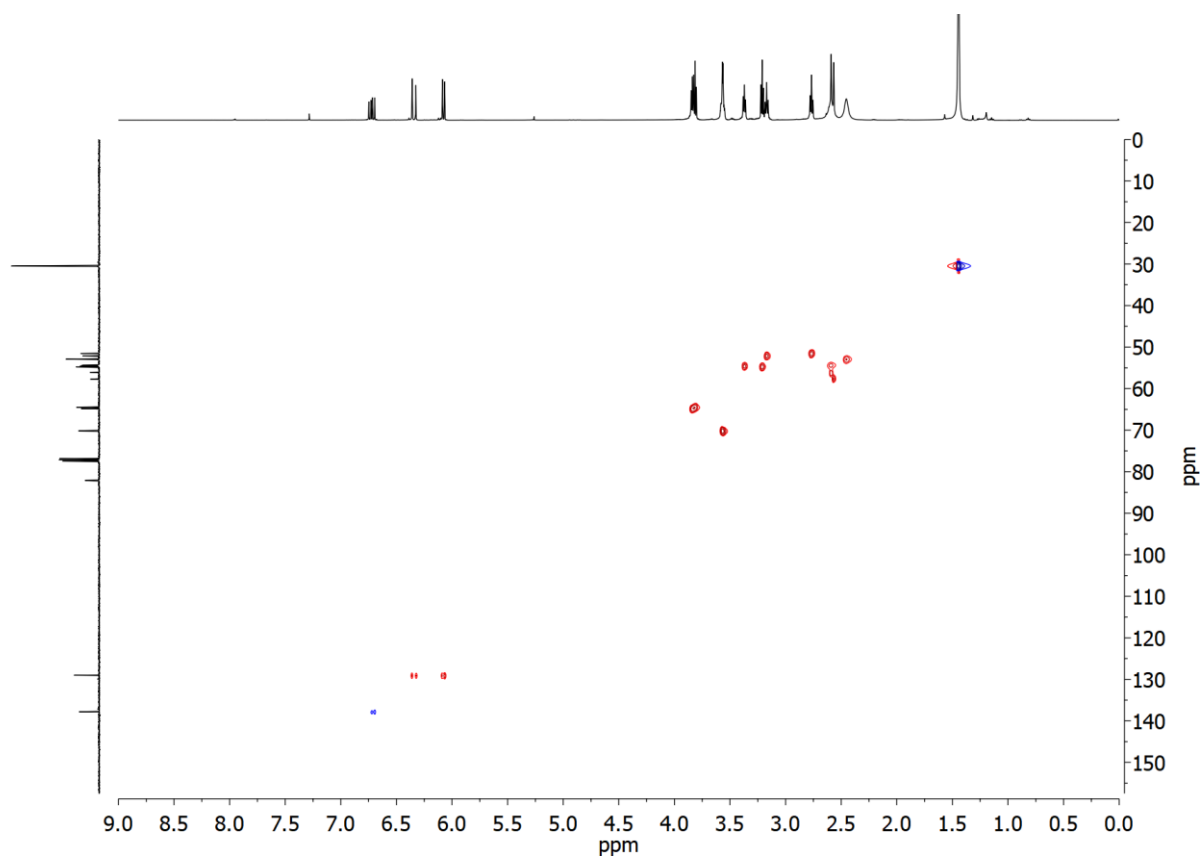


Figure S32. HSQC NMR (500 MHz and 126 MHz, CDCl_3) spectrum of **16**.

Compound 17:

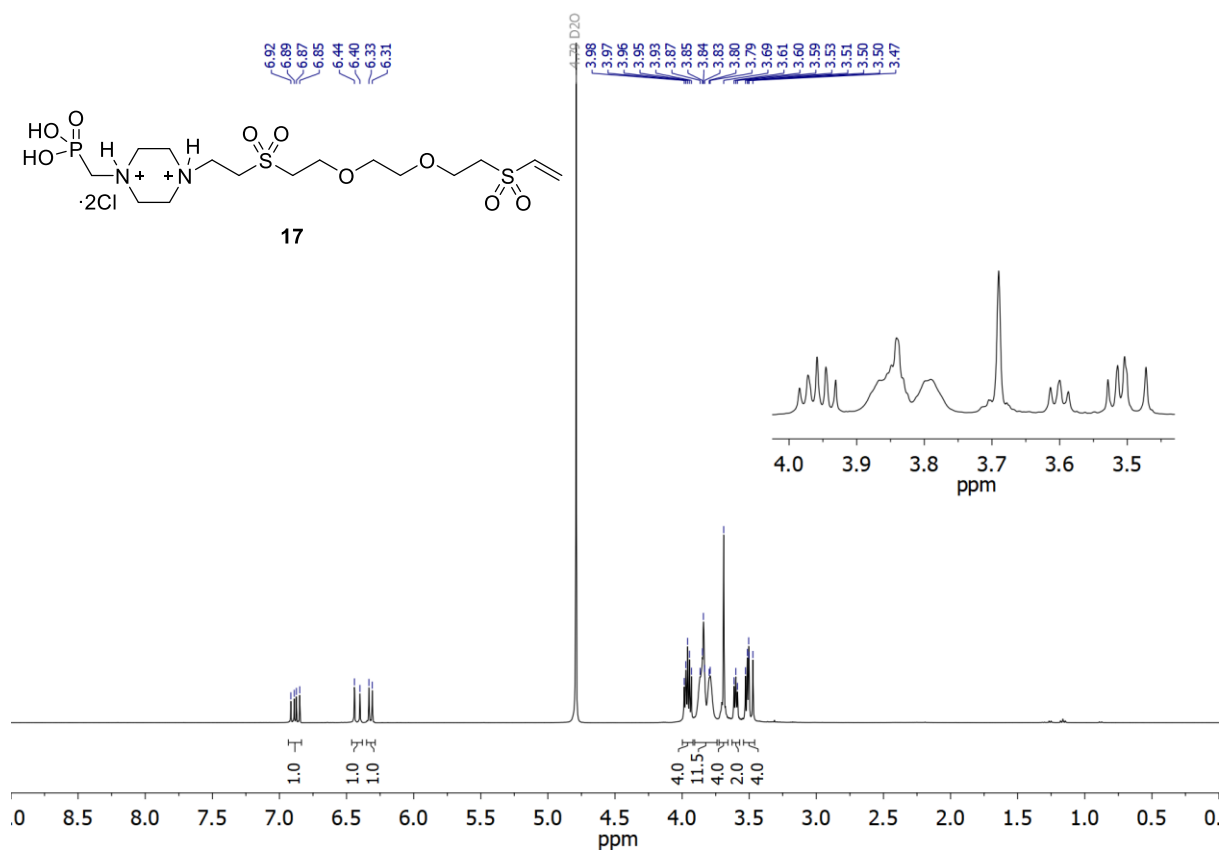


Figure S33. ¹H NMR (400 MHz, D₂O) spectrum of 17.

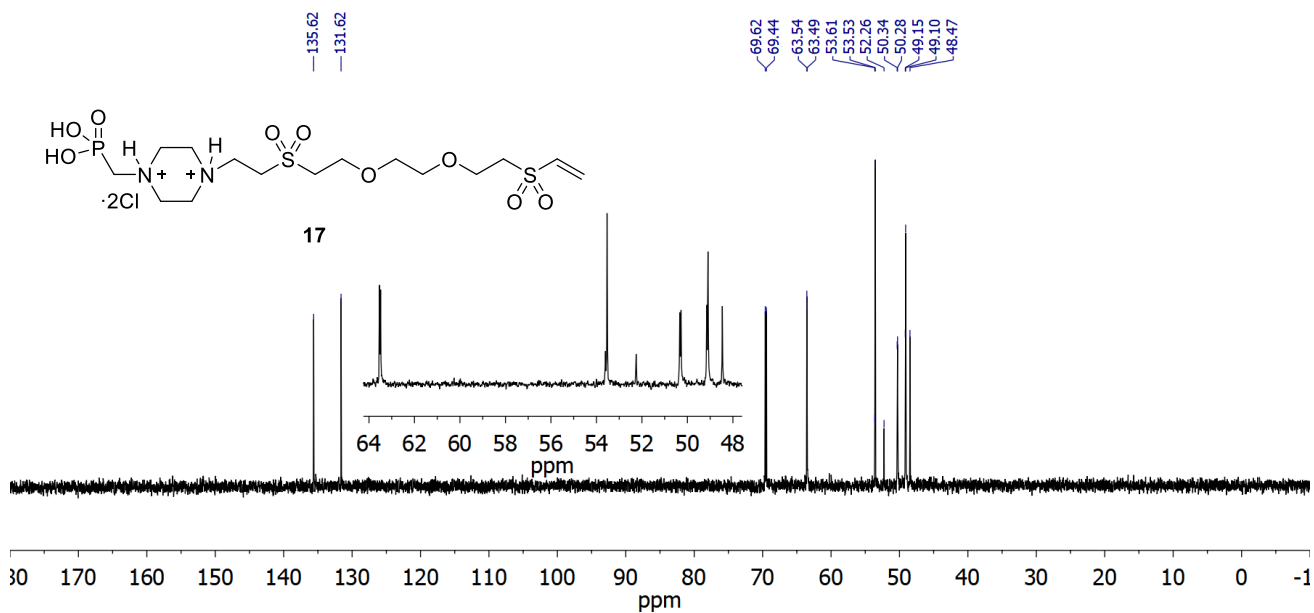


Figure S34. ¹³C NMR (101 MHz, D₂O) spectrum of 17.

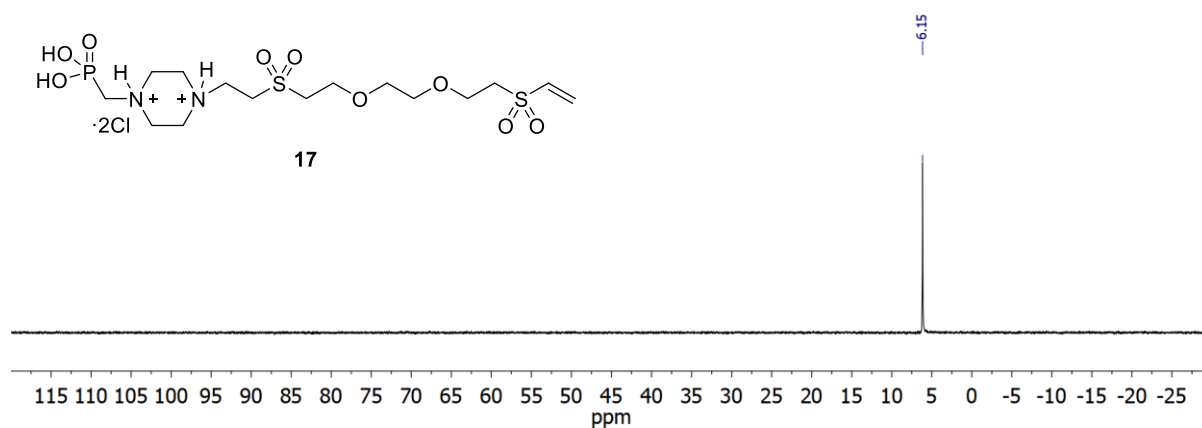


Figure S35. ^{31}P NMR (162 MHz, D_2O) spectrum of **17**.

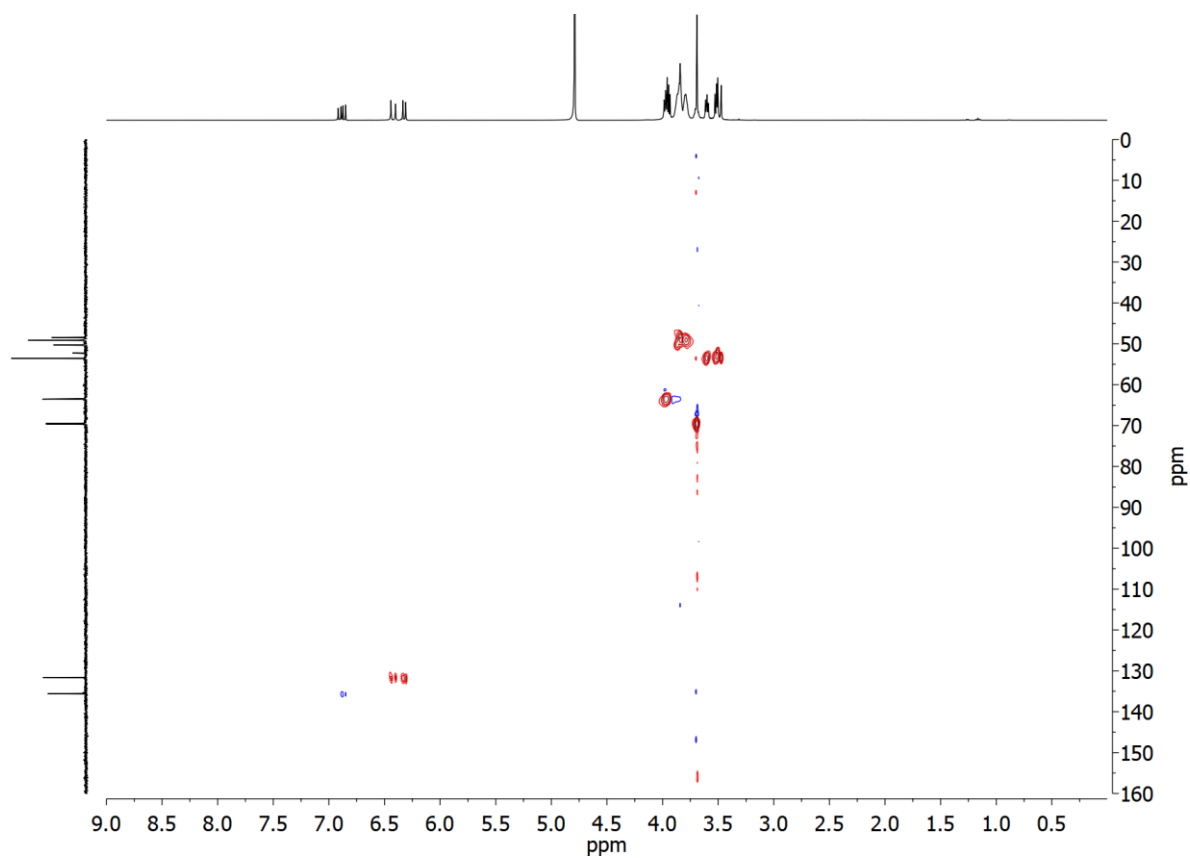


Figure S36. HSQC NMR (400 MHz and 101 MHz, D_2O) spectrum of **17**.

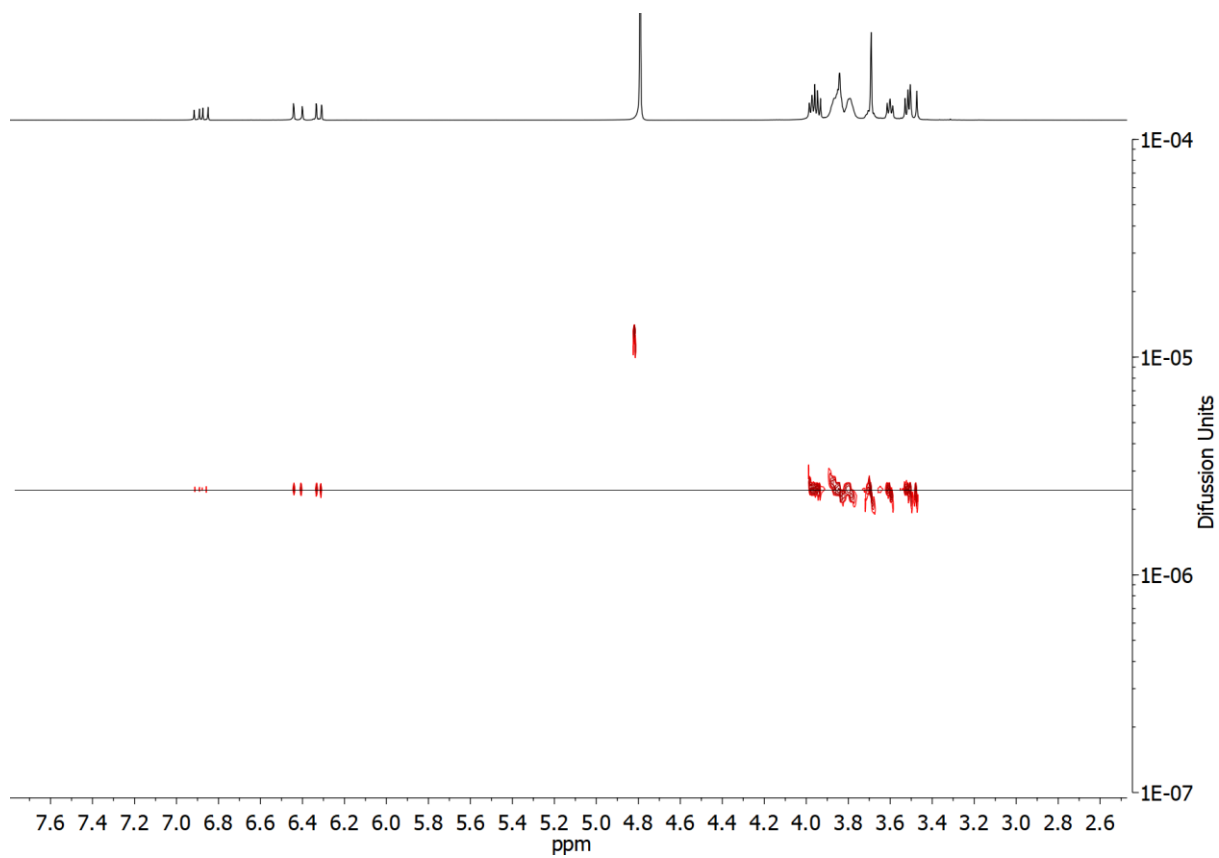


Figure S37. DOSY NMR (500 MHz, D₂O) spectrum of **17**.

Compound 20a:

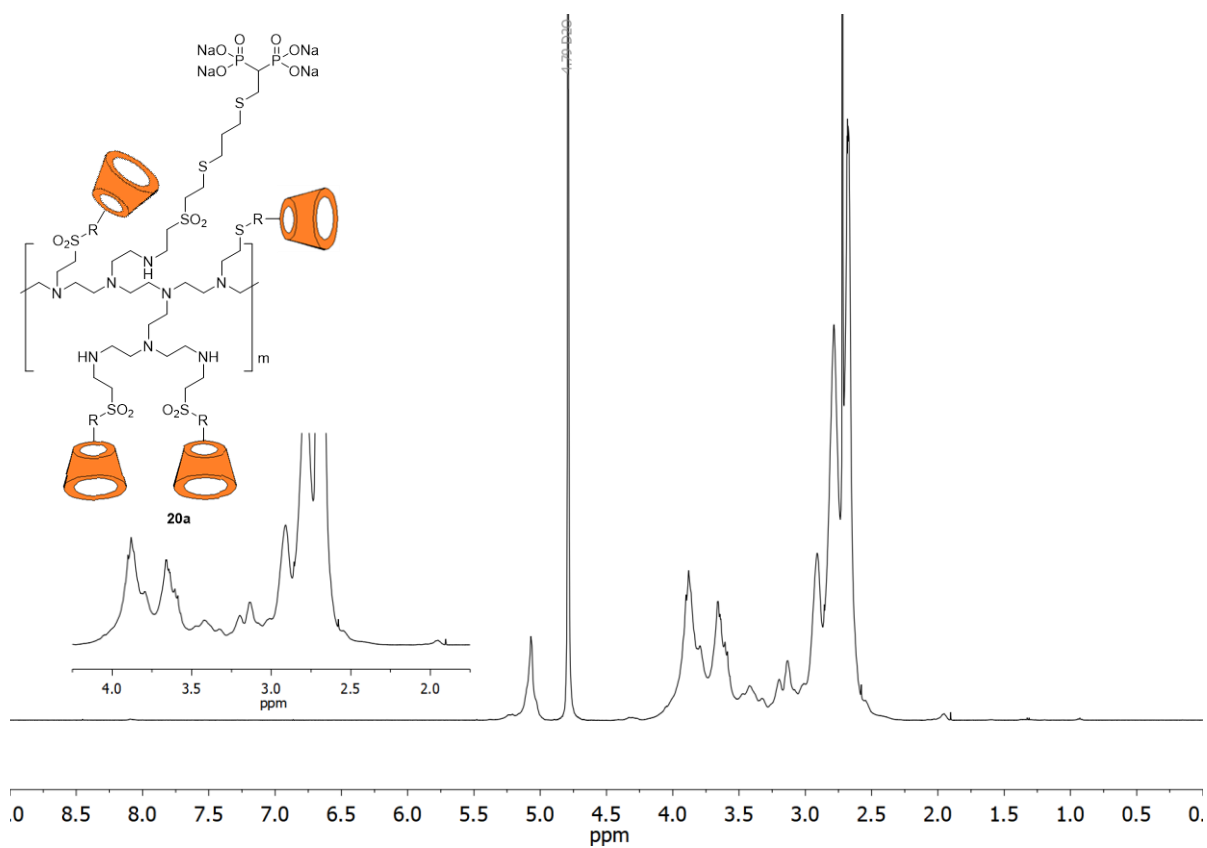


Figure S38. ^1H NMR (500 MHz, $\text{D}_2\text{O}/\text{DMSO-}d_6$) spectrum of 20a.

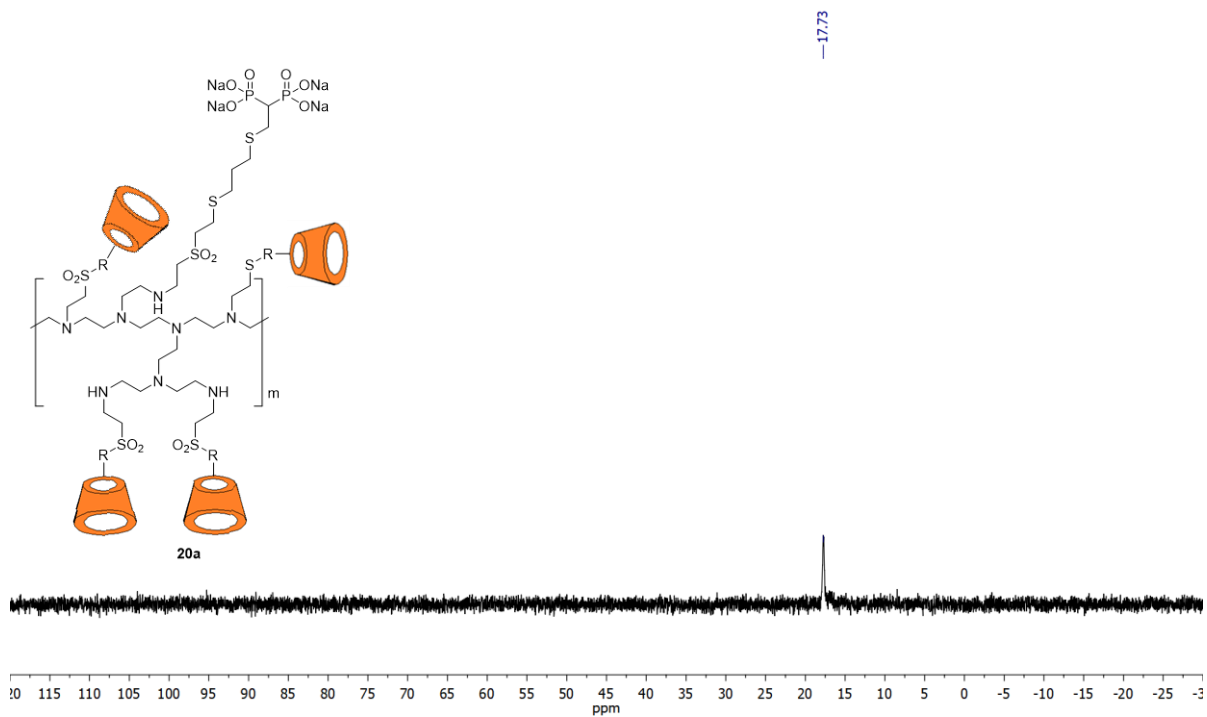


Figure S39. ^{31}P NMR (202 MHz, $\text{D}_2\text{O}/\text{DMSO-}d_6$) spectrum of 20a.

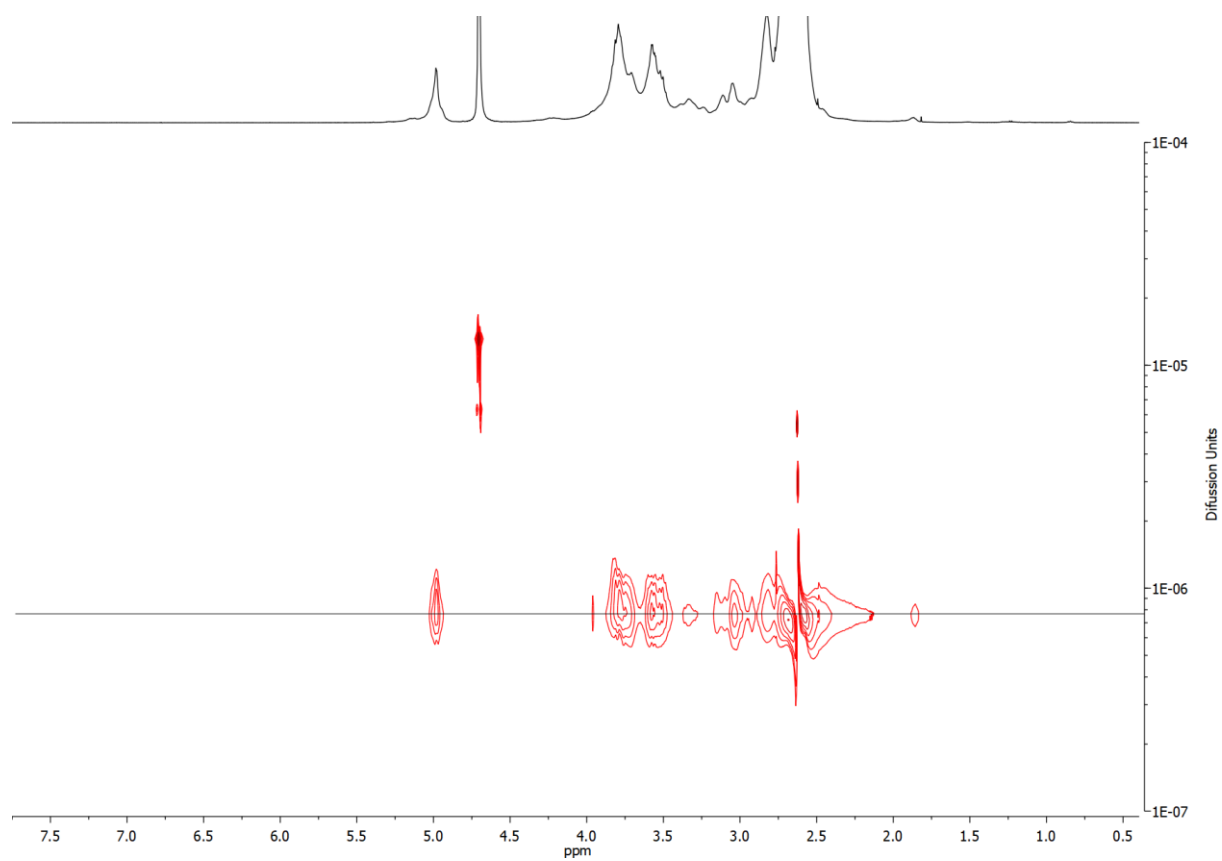


Figure S40. DOSY NMR (500 MHz, D₂O/DMSO-*d*₆) spectrum of **20a**.

Compound 20b:

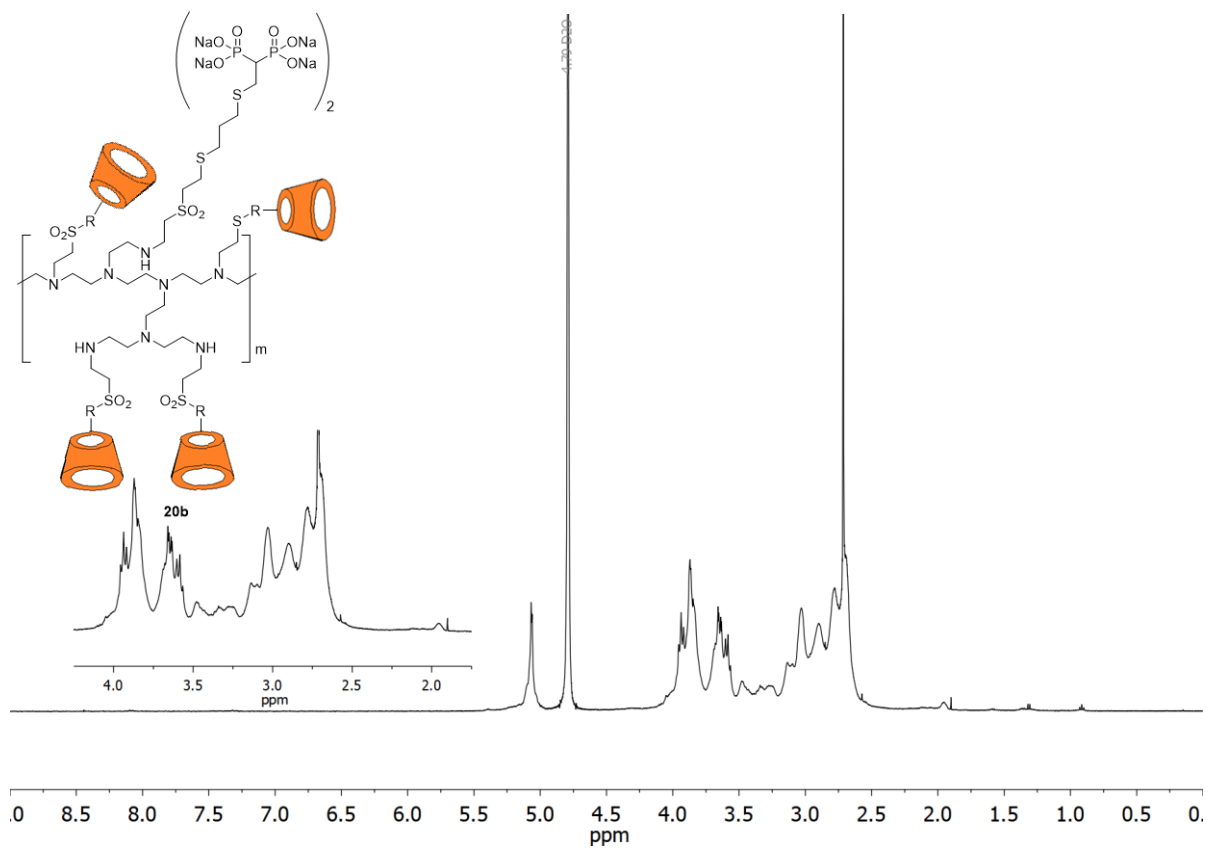


Figure S41. ¹H NMR (500 MHz, D₂O/DMSO-*d*₆) spectrum of 20b.

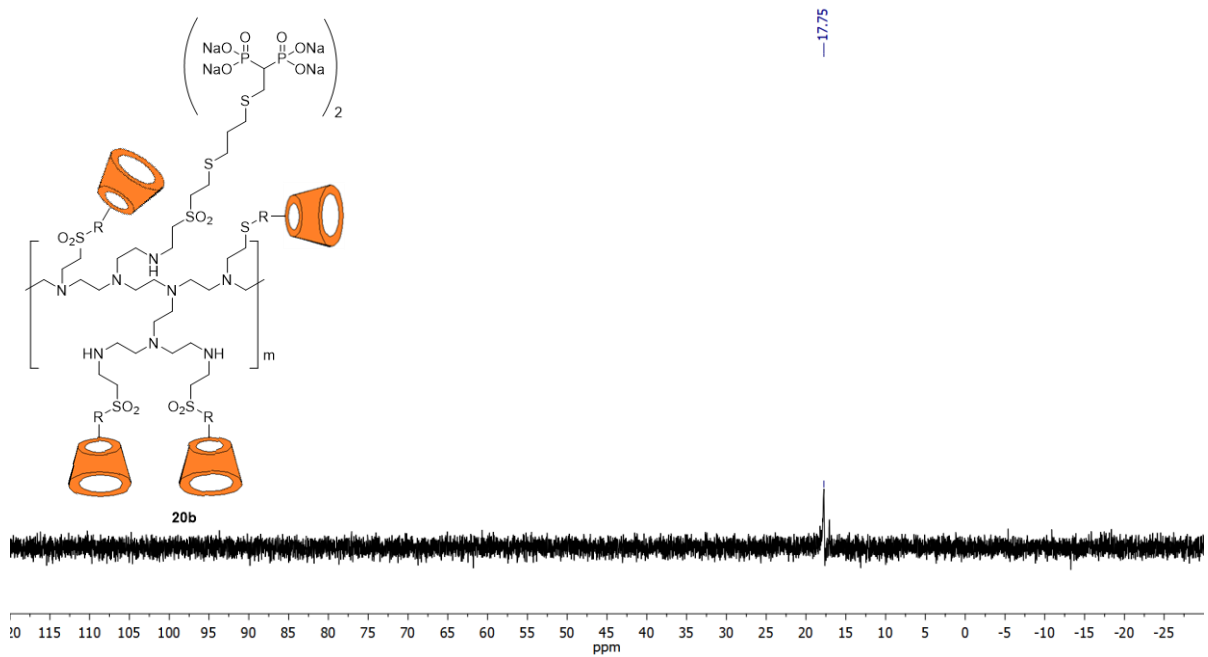


Figure S42. ³¹P NMR (162 MHz, D₂O/DMSO-*d*₆) spectrum of 20b.

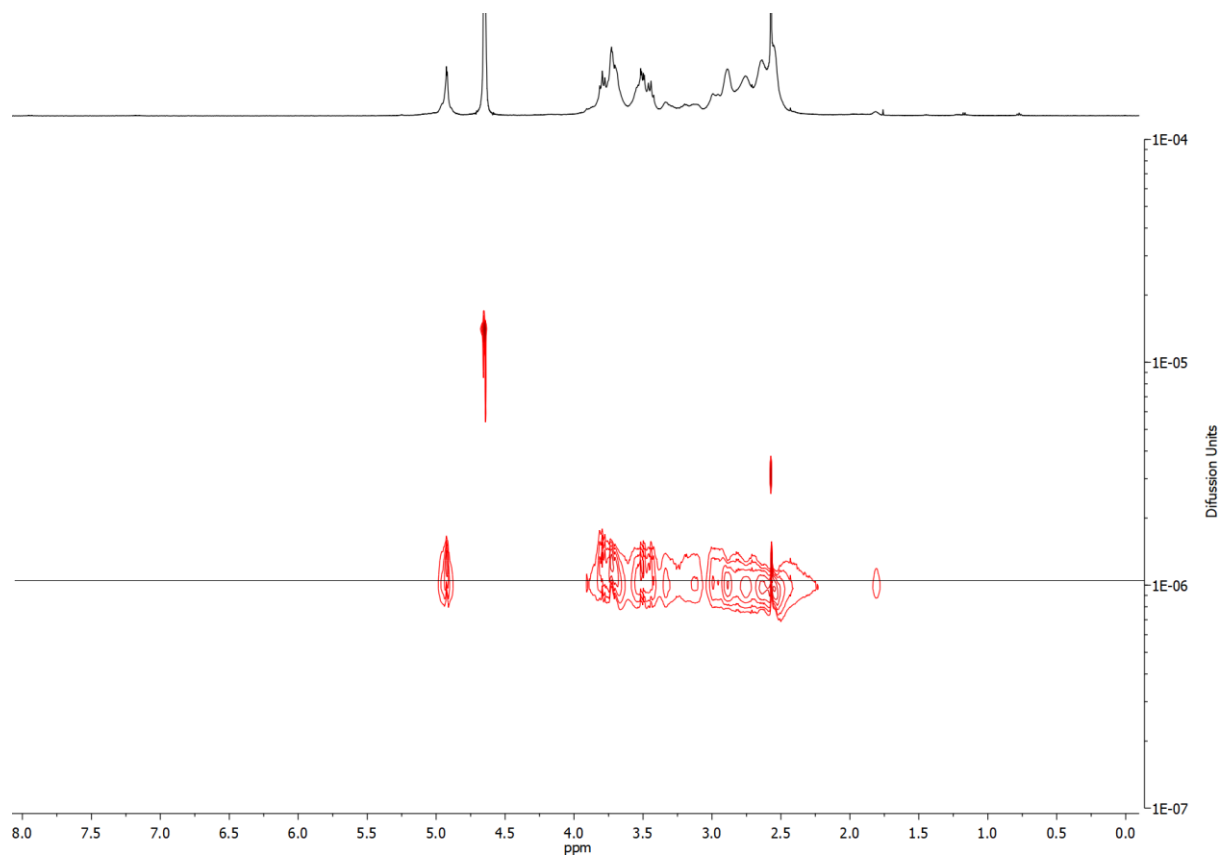


Figure S43. DOSY NMR (500 MHz, D₂O/DMSO-*d*₆) spectrum of **20b**.

Compound 21a:

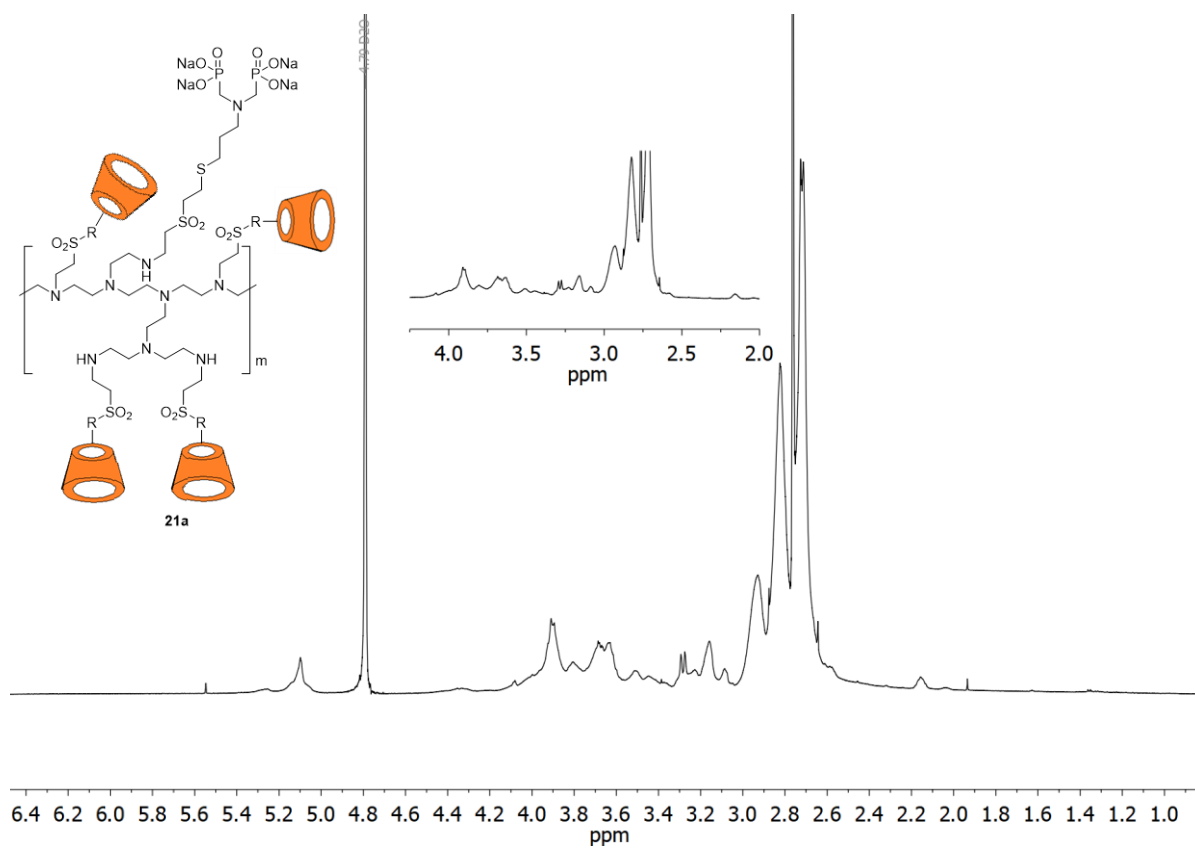


Figure S44. Partial ^1H NMR (600 MHz, $\text{D}_2\text{O}/\text{DMSO-}d_6$) spectrum of **21a**.

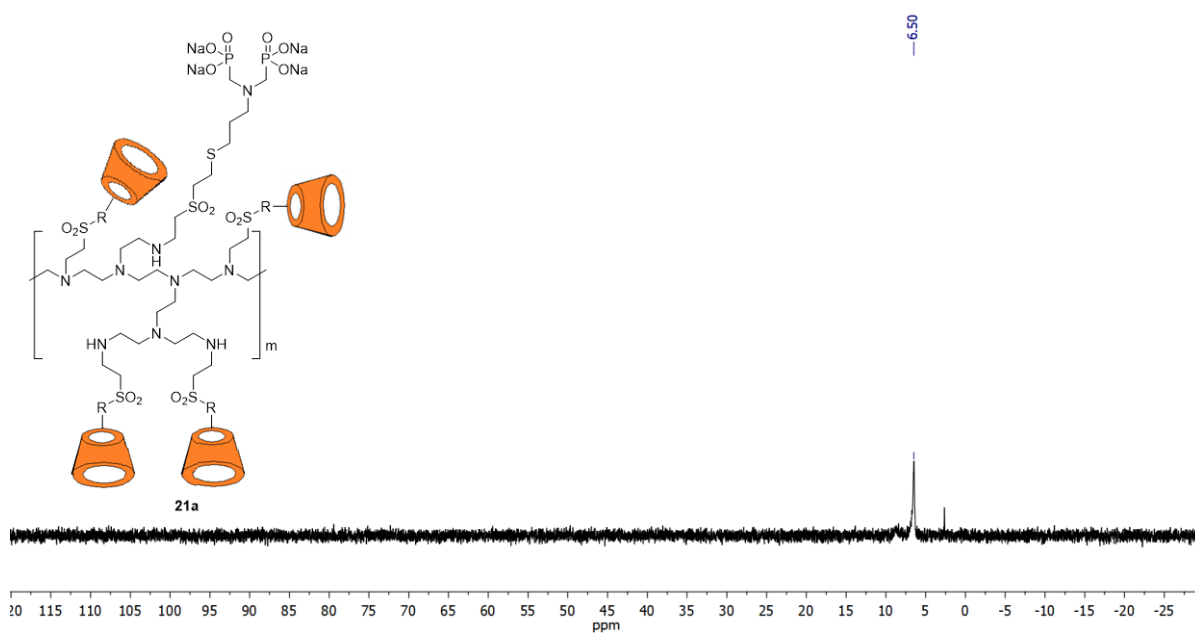


Figure S45. ^{31}P NMR (202 MHz, $\text{D}_2\text{O}/\text{DMSO-}d_6$) spectrum of **21a**.

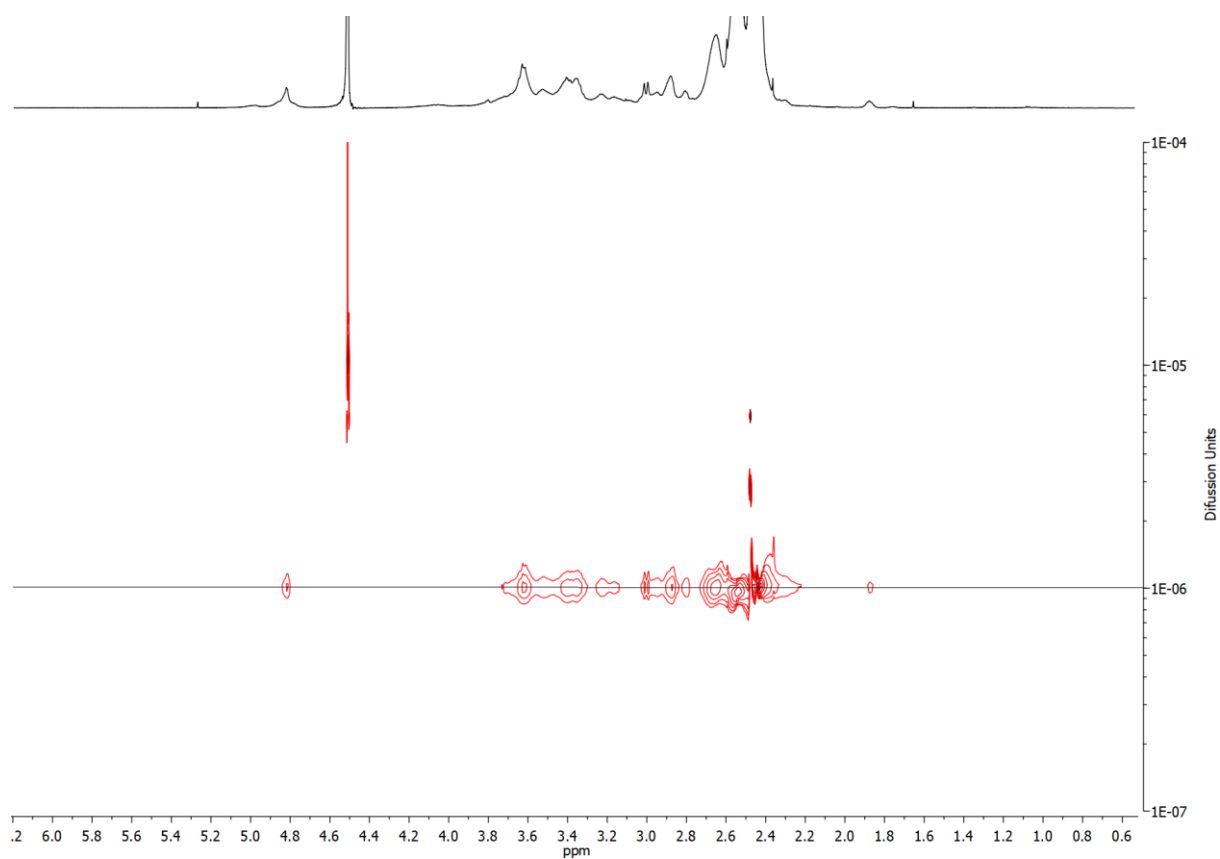


Figure S45. DOSY NMR (600 MHz, D₂O/DMSO-*d*₆) spectrum of **21a**.

Compound 21b:

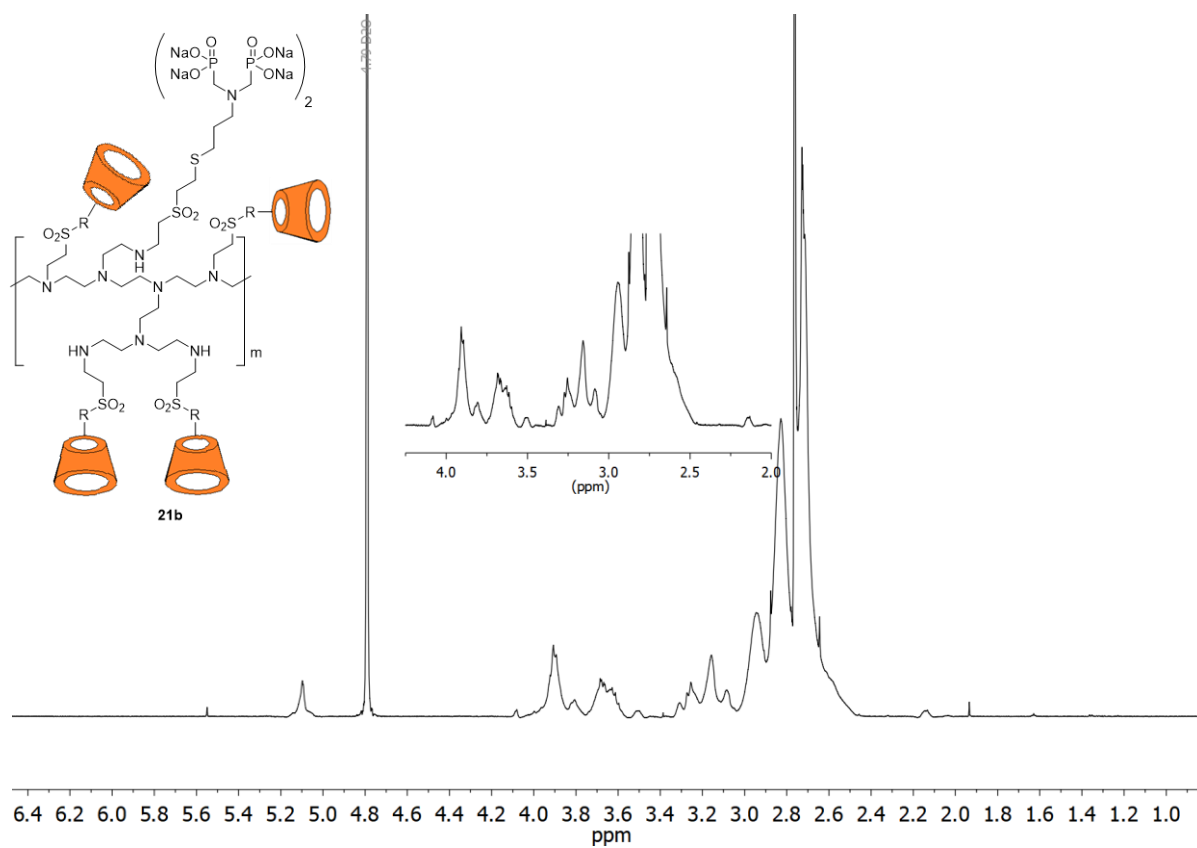


Figure S47. Partial ^1H NMR (600 MHz, $\text{D}_2\text{O}/\text{DMSO}-d_6$) spectrum of 21b.

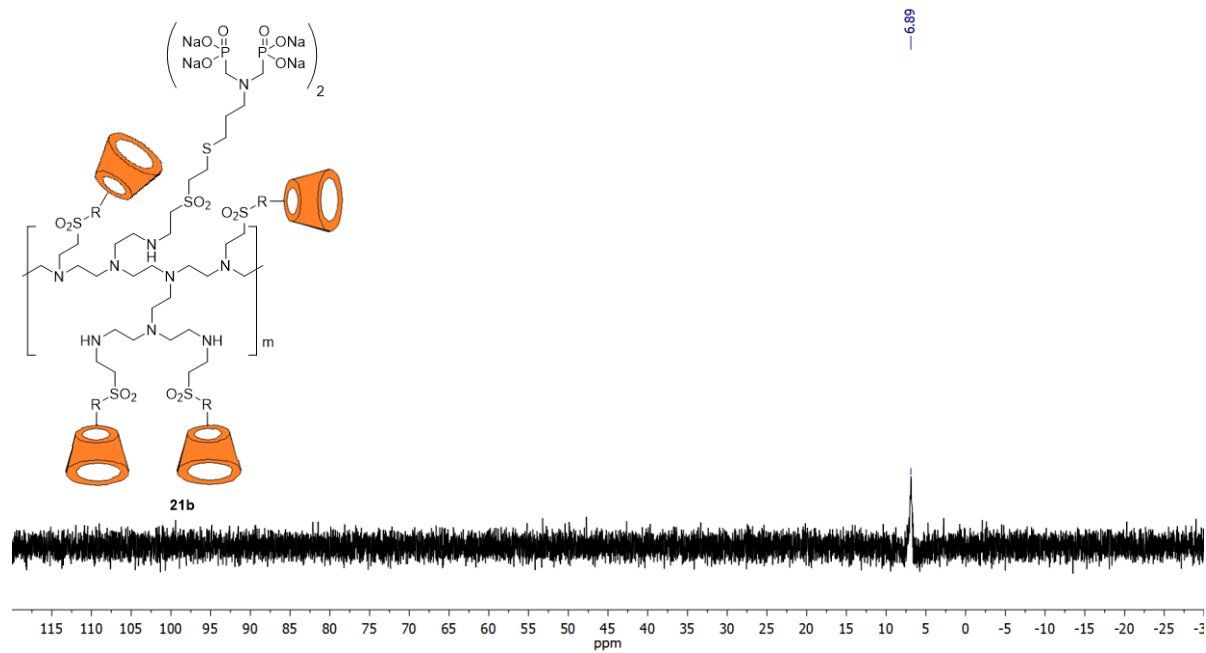


Figure S48. ^{31}P NMR (202 MHz, $\text{D}_2\text{O}/\text{DMSO}-d_6$) spectrum of 21b.

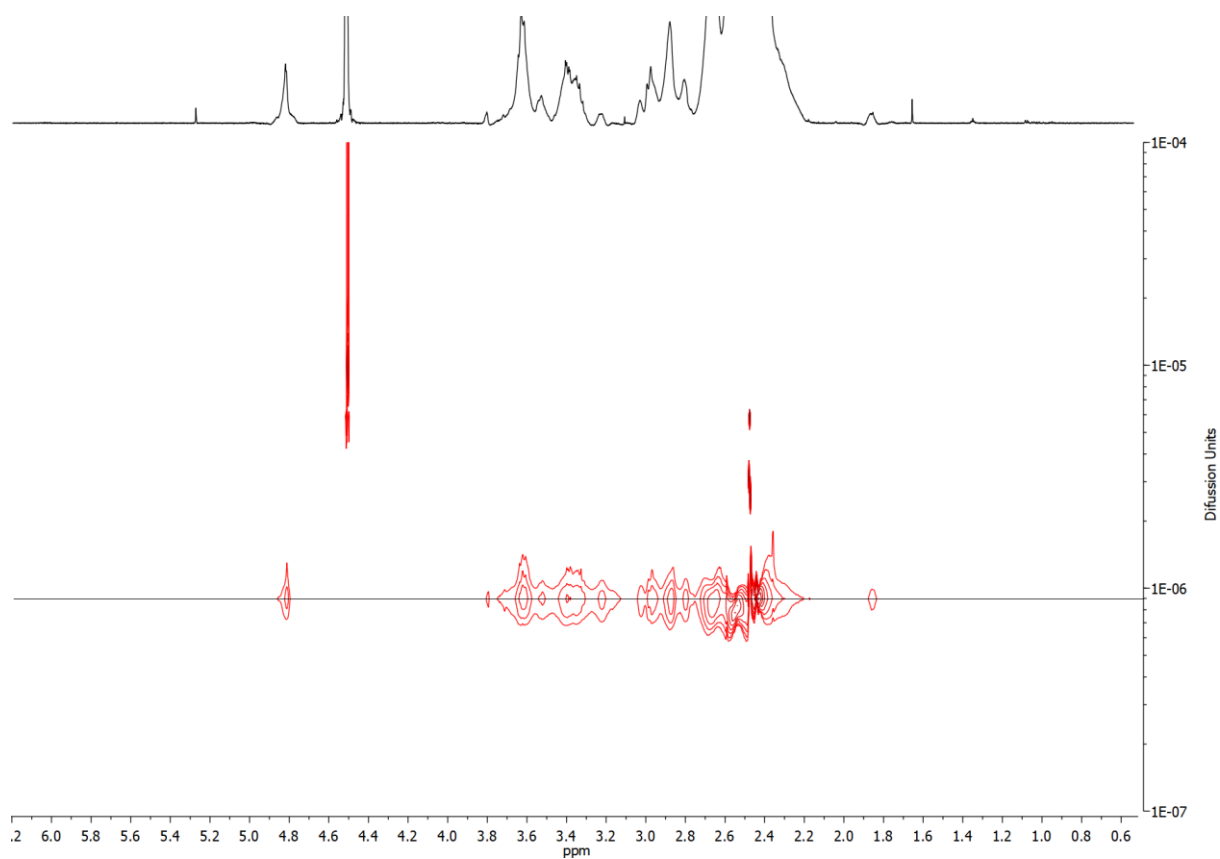


Figure S49. DOSY NMR (600 MHz, D₂O/DMSO-*d*₆) spectrum of **21b**.

Compound 22a:

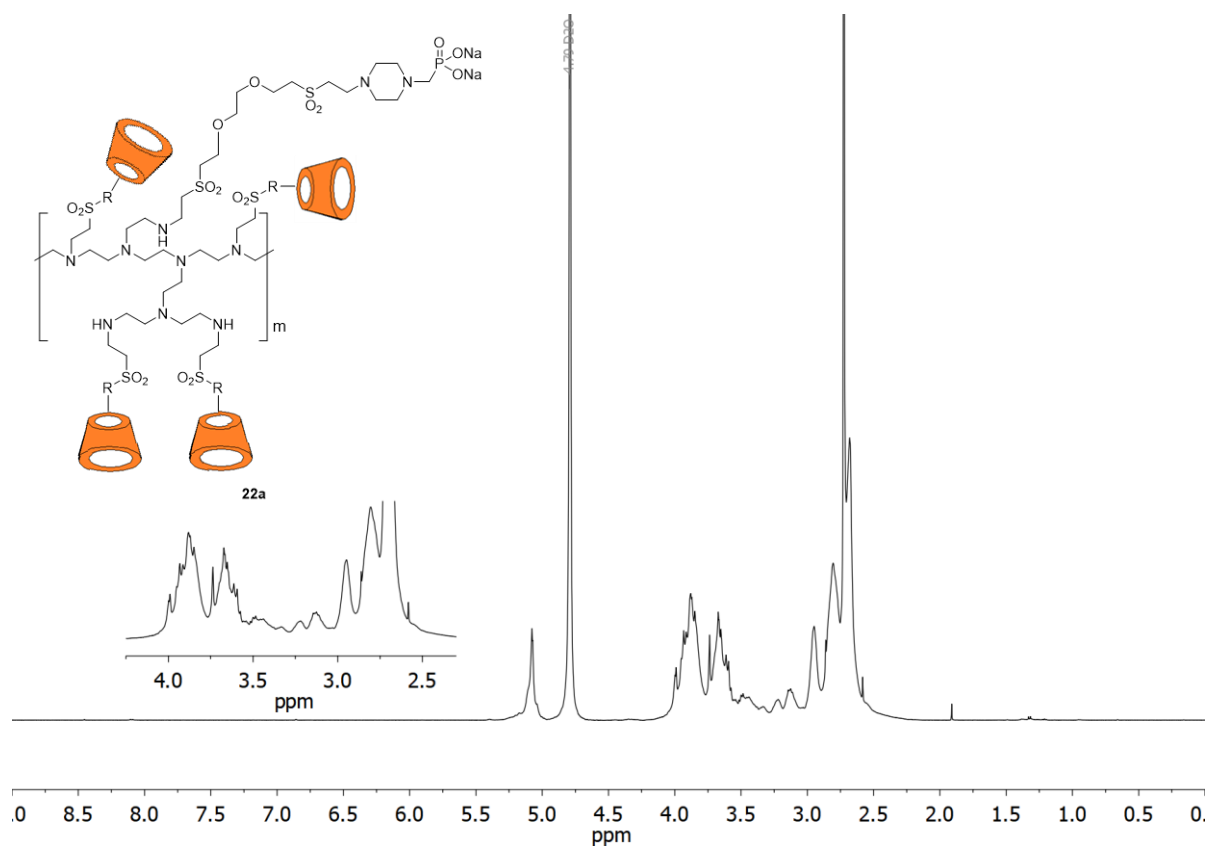


Figure S50. ^1H NMR (500 MHz, $\text{D}_2\text{O}/\text{DMSO-}d_6$) spectrum of 22a.

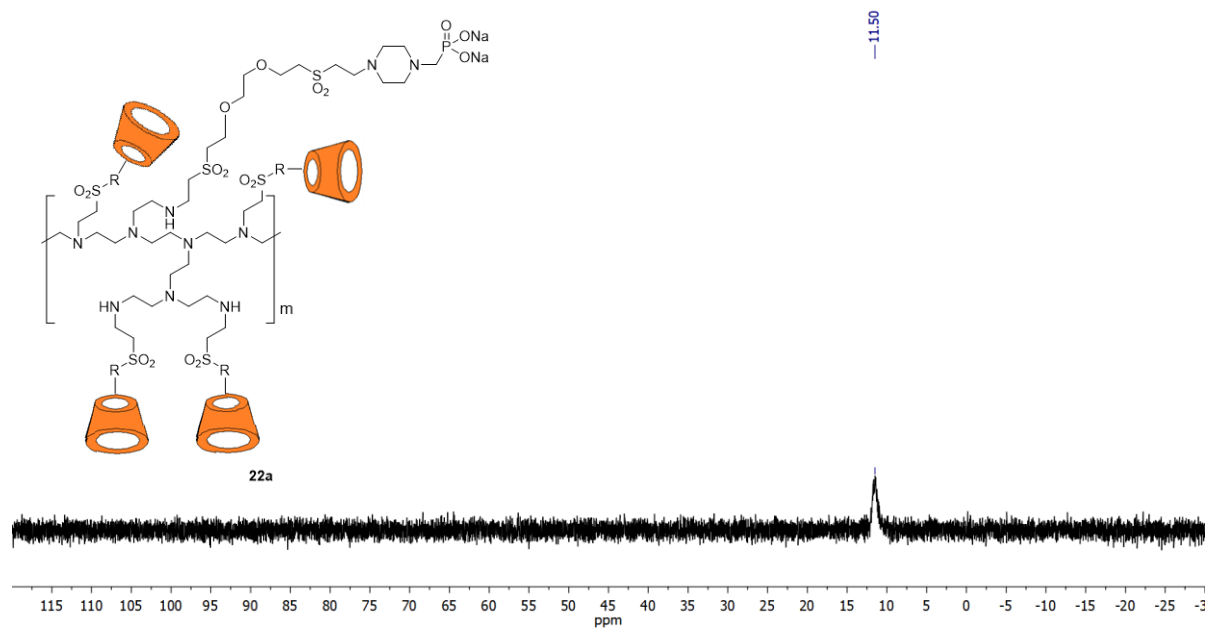


Figure S51. ^{31}P NMR (202 MHz, $\text{D}_2\text{O}/\text{DMSO-}d_6$) spectrum of 22a.

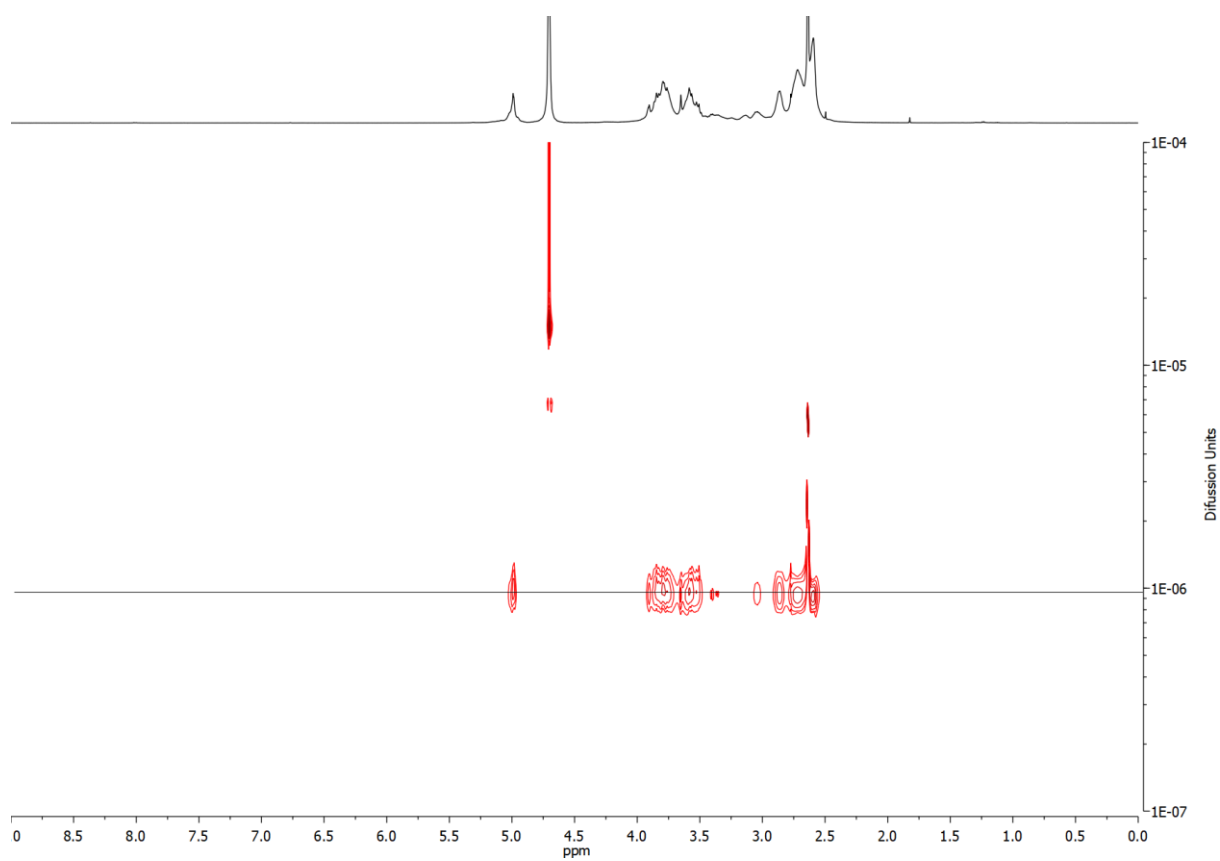


Figure S52. DOSY NMR (500 MHz, D₂O/DMSO-*d*₆) spectrum of **22a**.

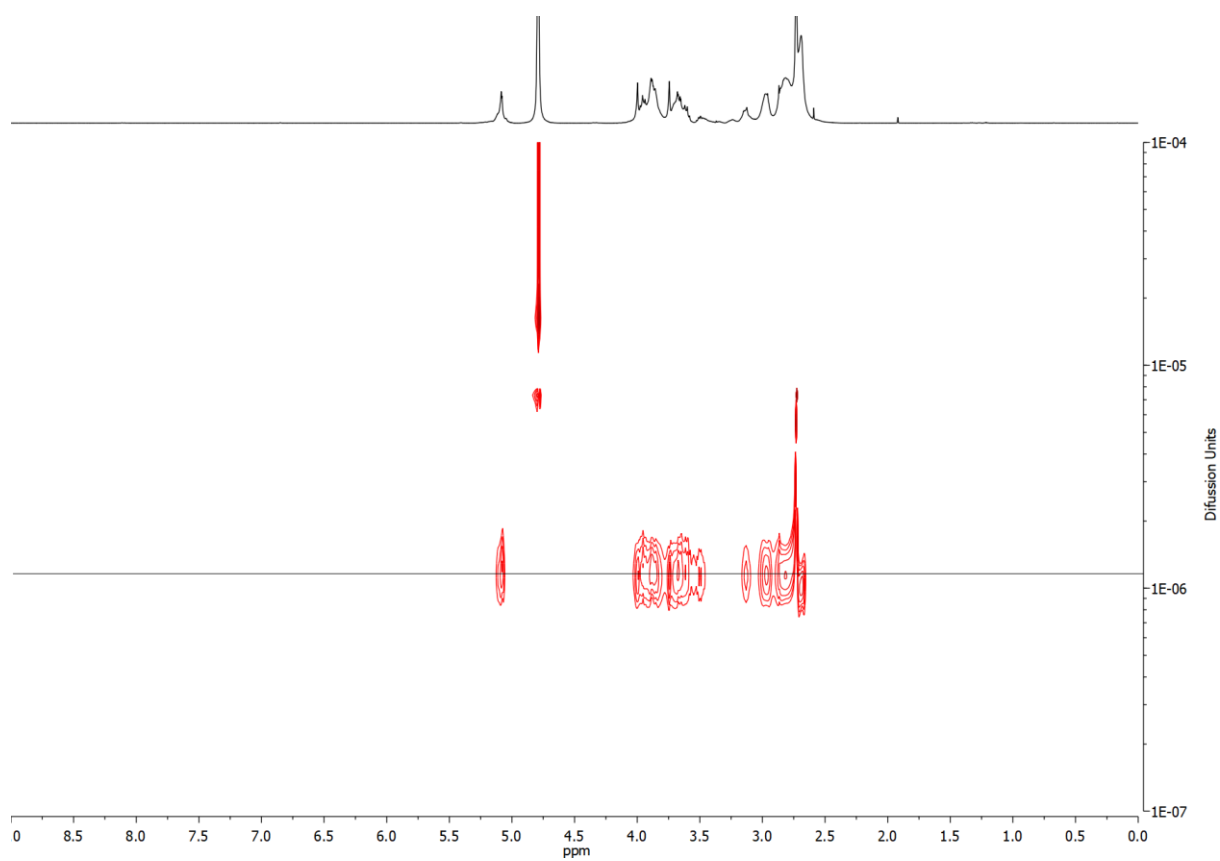


Figure S55. DOSY NMR (500 MHz, D₂O/DMSO-*d*₆) spectrum of **22b**.

3. HRMS spectra of key compounds

Compound 5

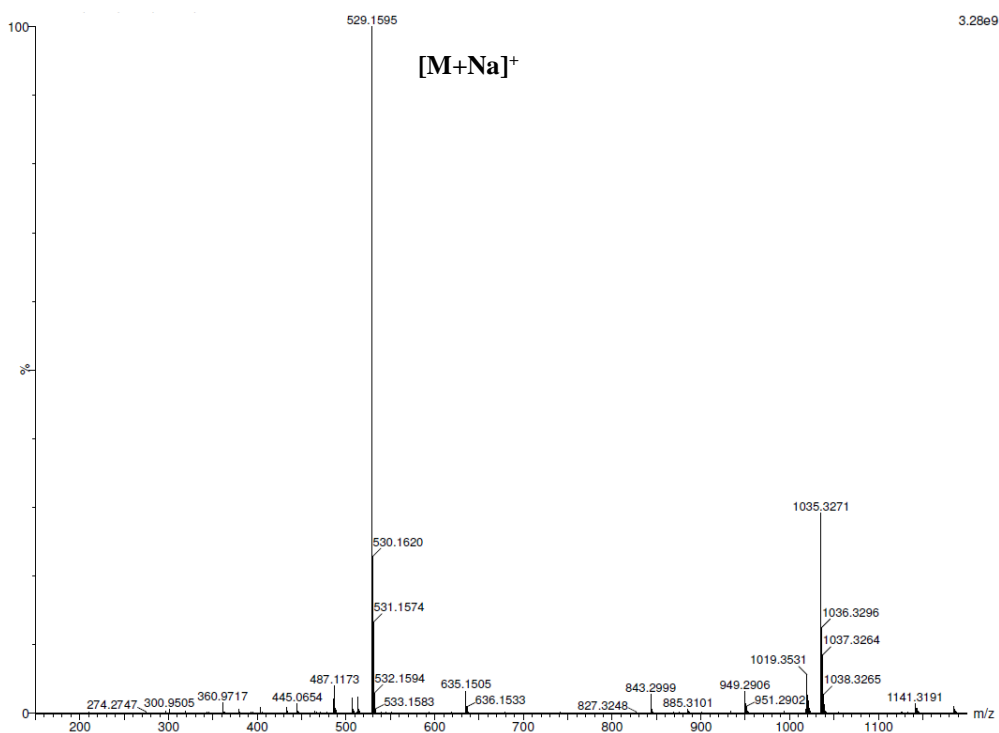


Figure S56. HRMS (ESI⁺) spectrum of 5.

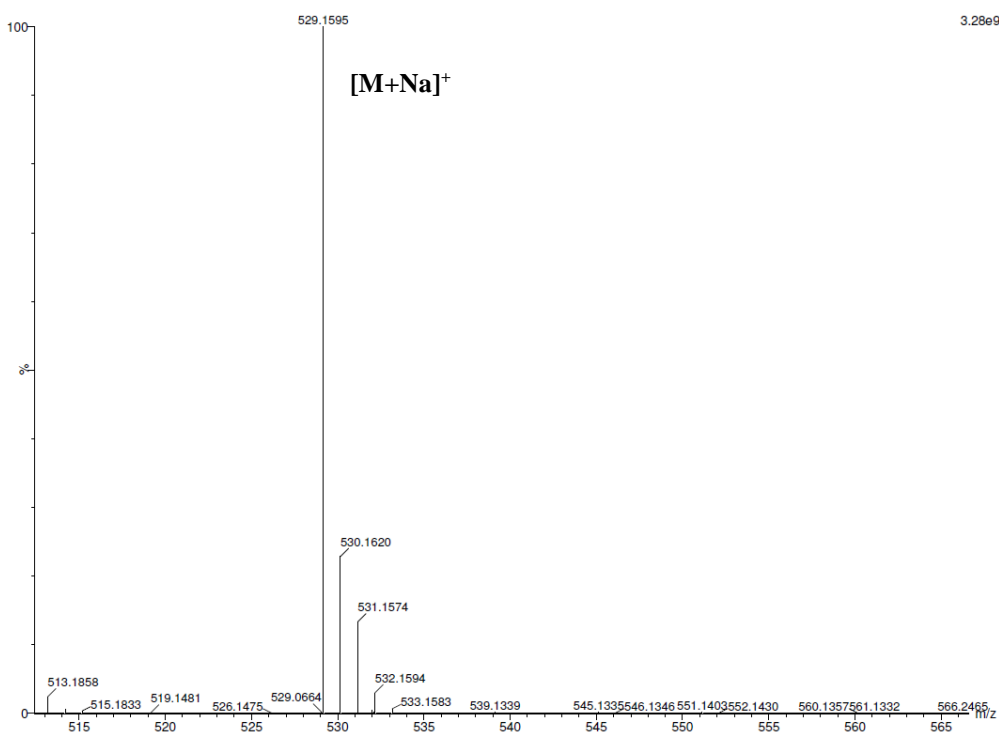


Figure S57. Partial HRMS (ESI⁺) spectrum of 5.

Compound 7

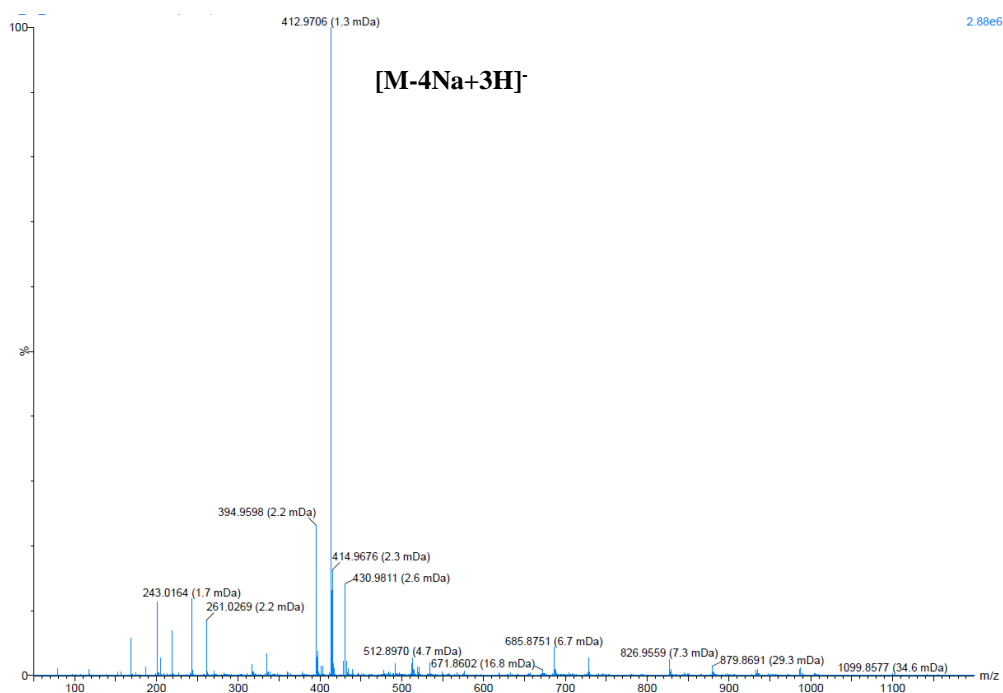


Figure S58. HRMS (ESI-) spectrum of **7** (performed using 0.1% of formic acid).

Compound 9

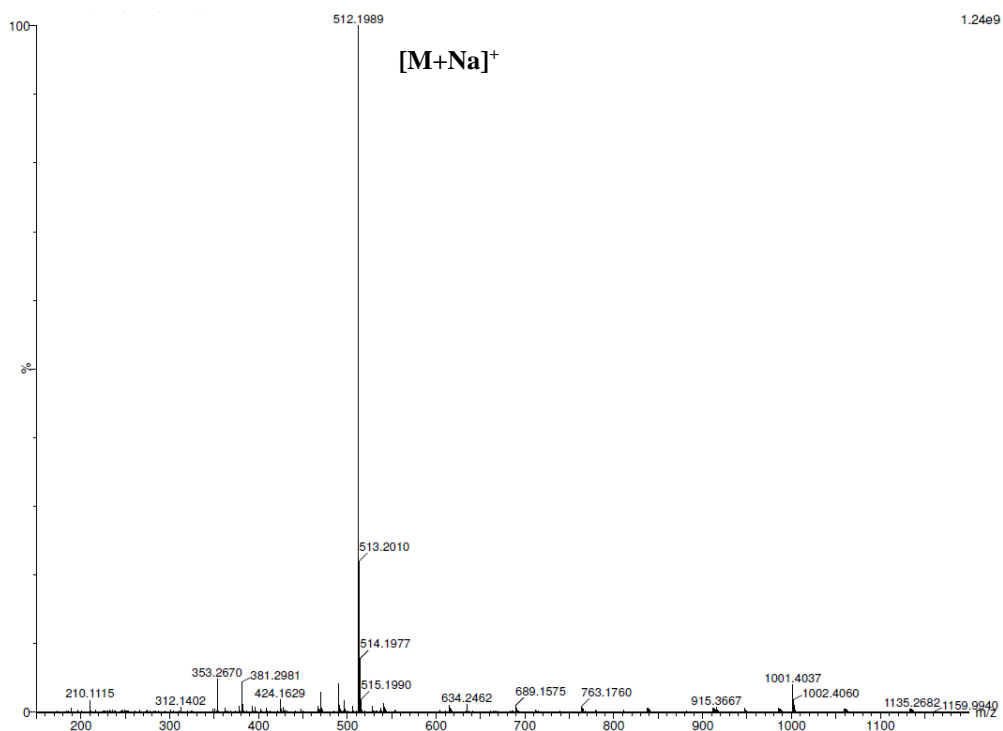


Figure S59. HRMS (ESI+) spectrum of **9**.

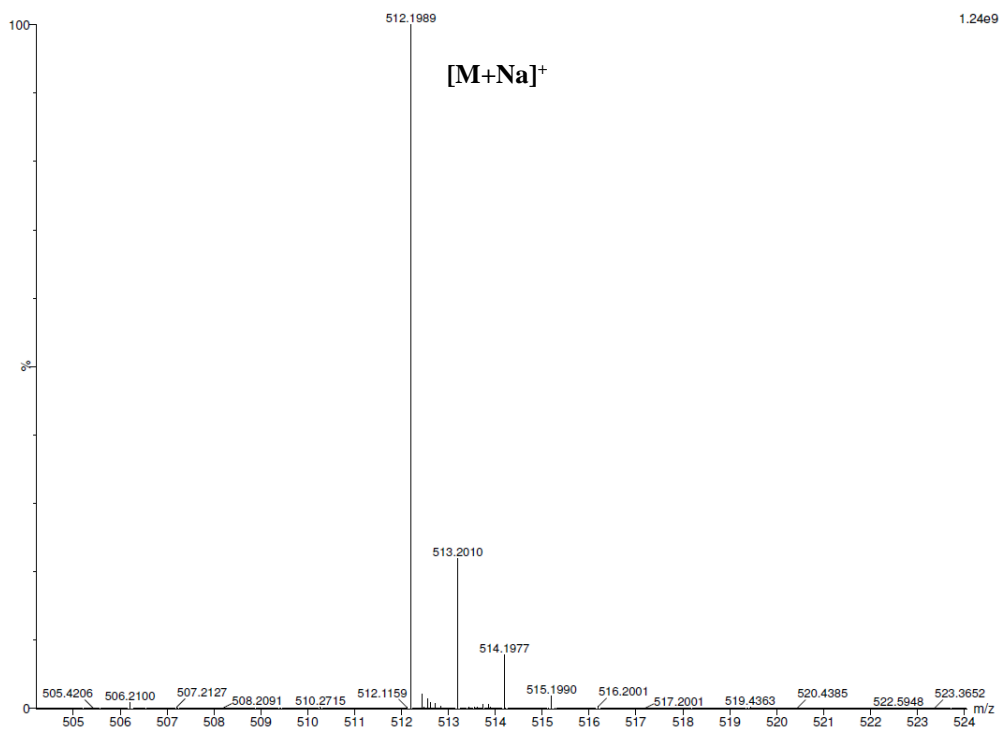


Figure S60. Partial HRMS (ESI⁺) spectrum of **9**.

Compound 11

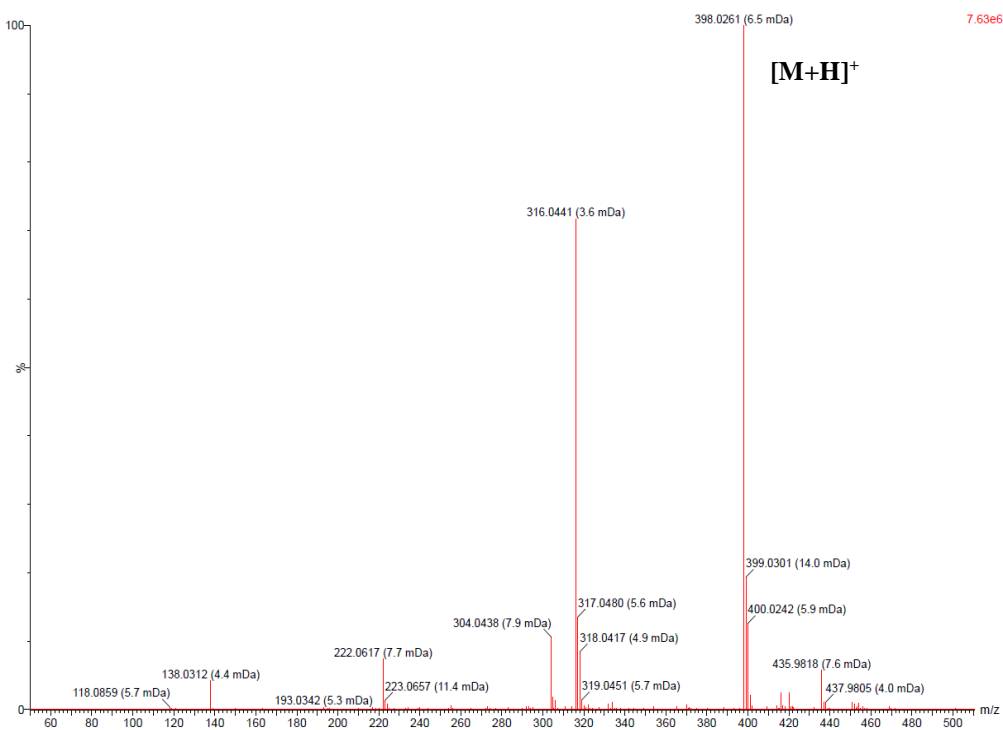


Figure S61. HRMS (ESI⁺) spectrum of **11** (performed using 0.1% of formic acid).

Compound 13

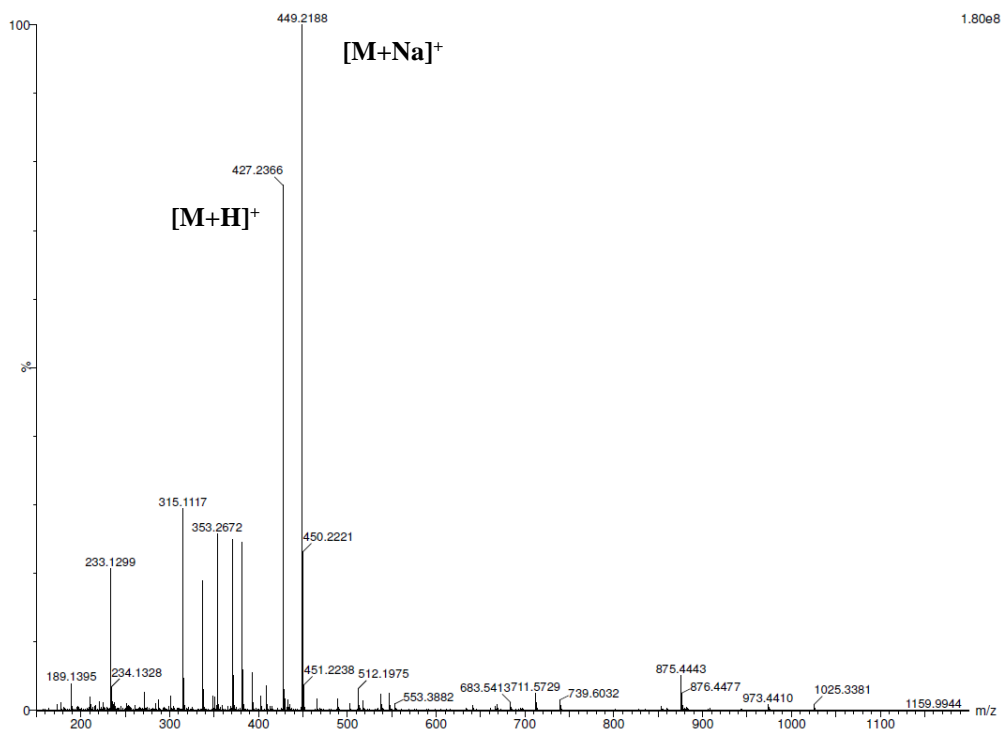


Figure S62. HRMS (ESI⁺) spectrum of 13.

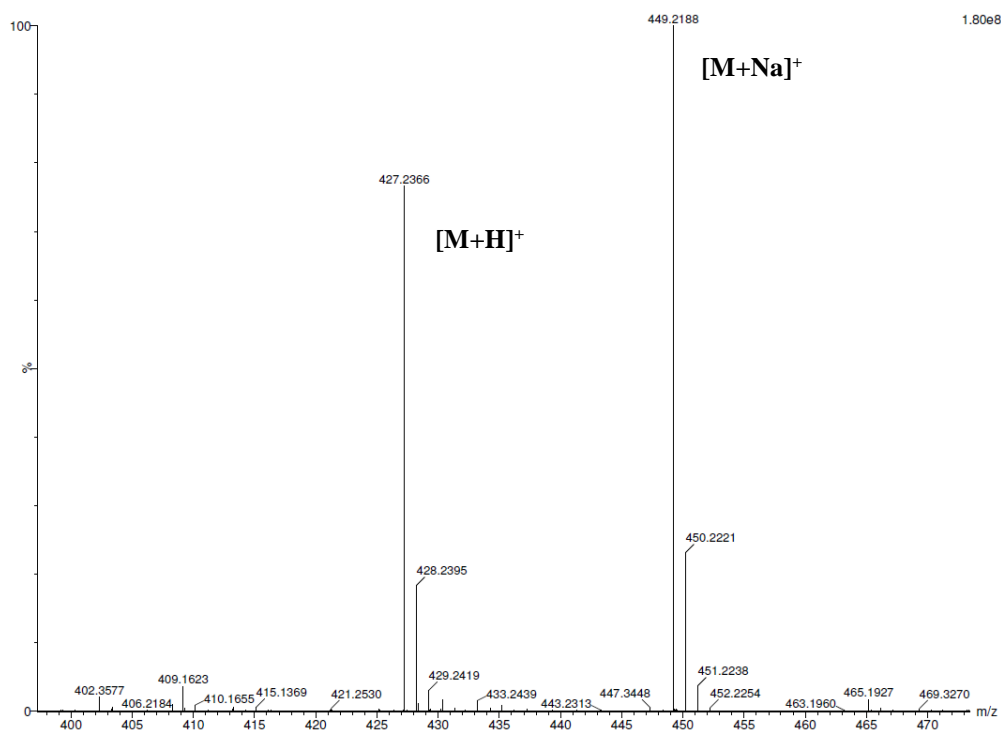


Figure S63. Partial HRMS (ESI⁺) spectrum of 13.

Compound 14

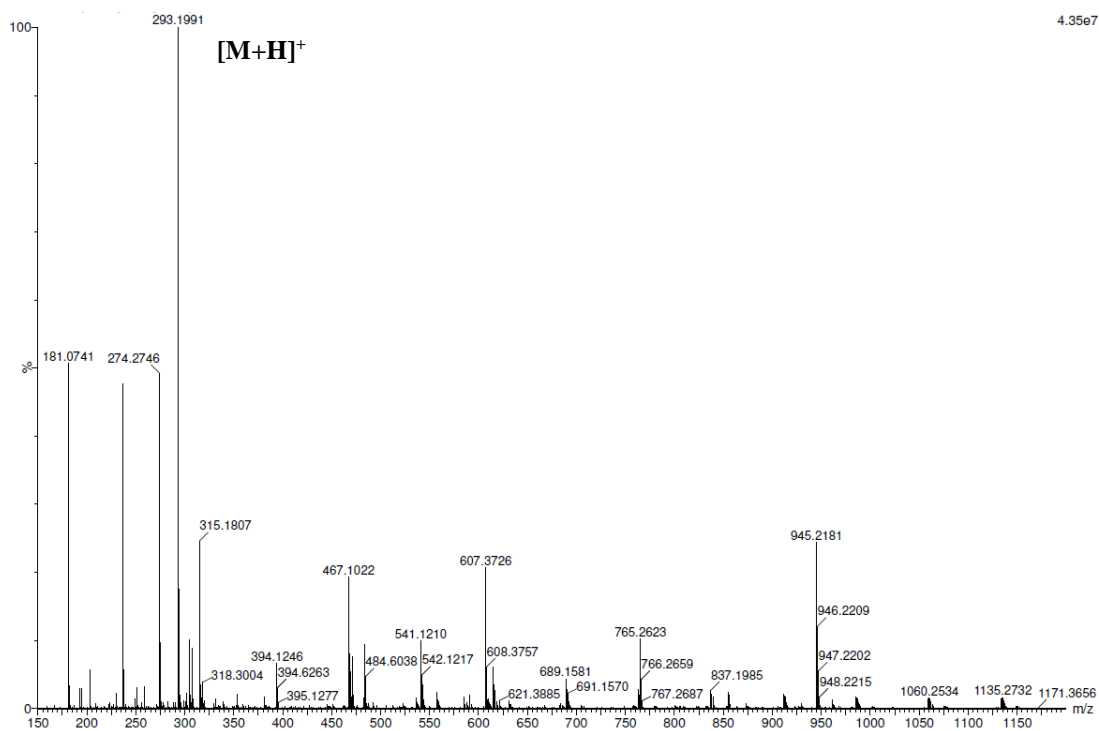


Figure S64. HRMS (ESI⁺) spectrum of 14.

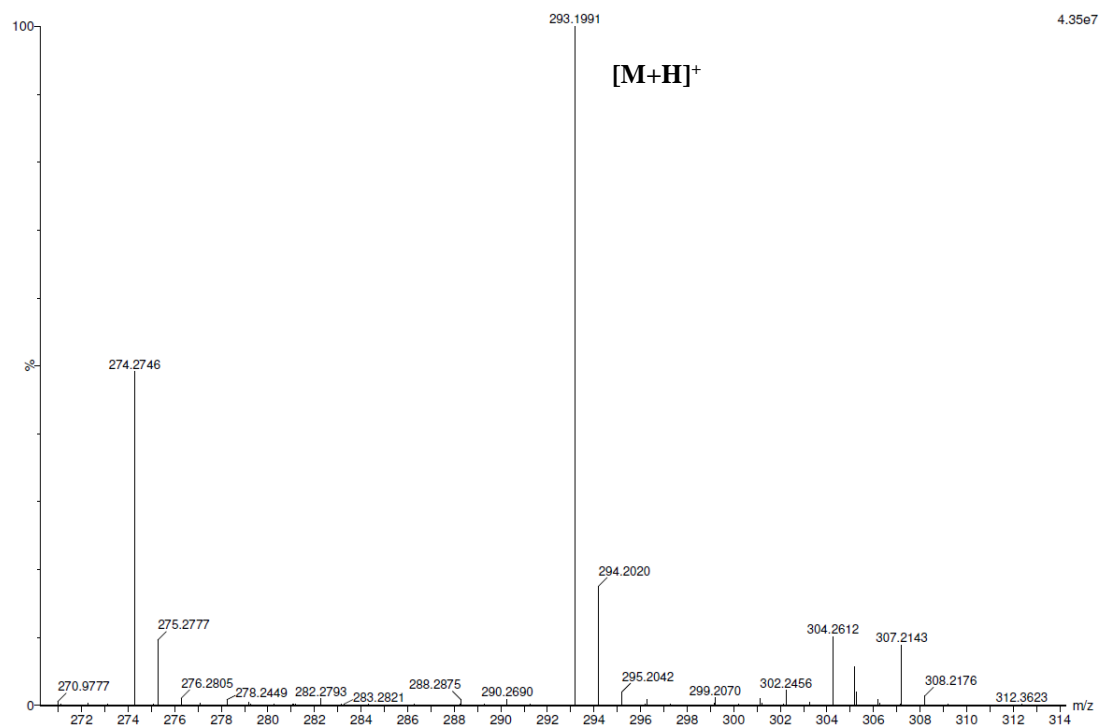


Figure S65. Partial HRMS (ESI⁺) spectrum of 14.

Compound 16

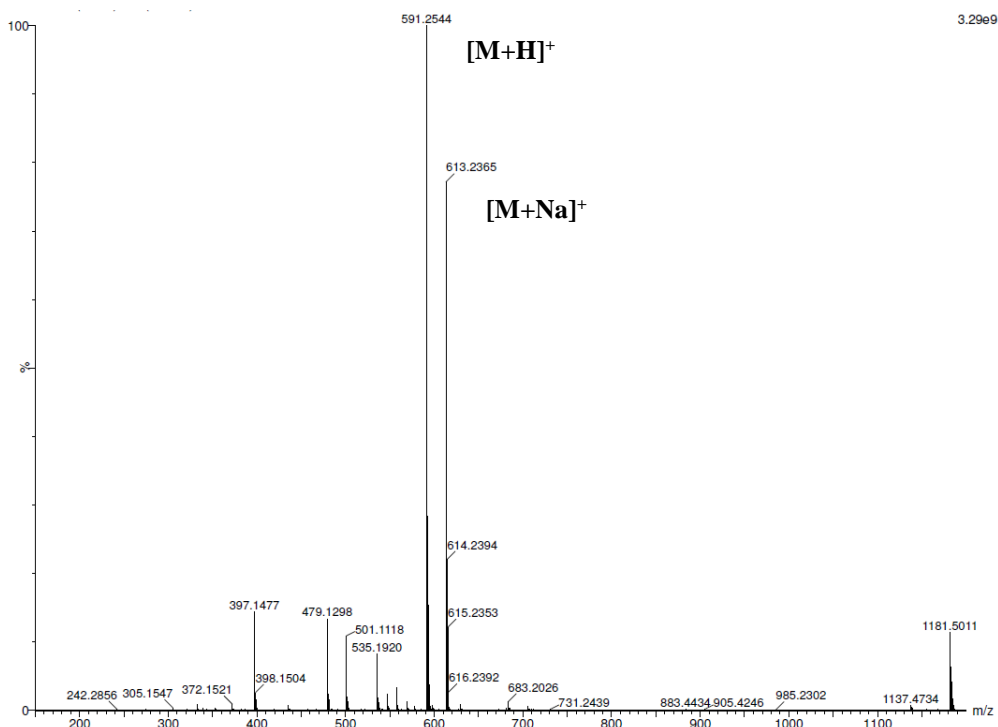


Figure S66. HRMS (ESI⁺) spectrum of 16.

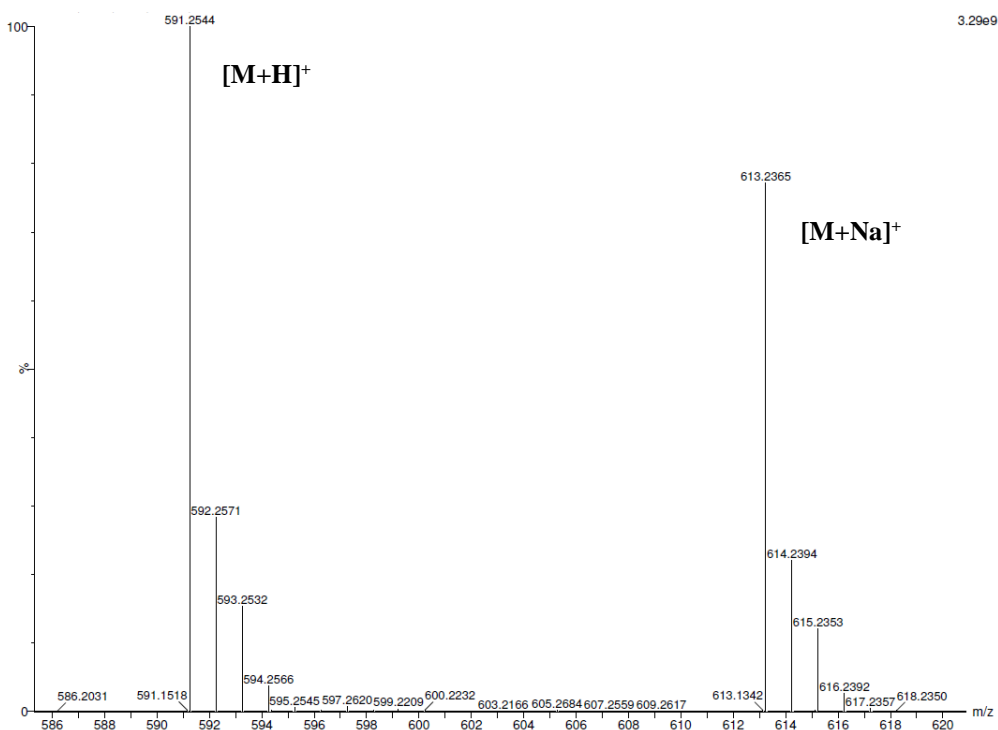


Figure S67. Partial HRMS (ESI⁺) spectrum of 16.

Compound 17

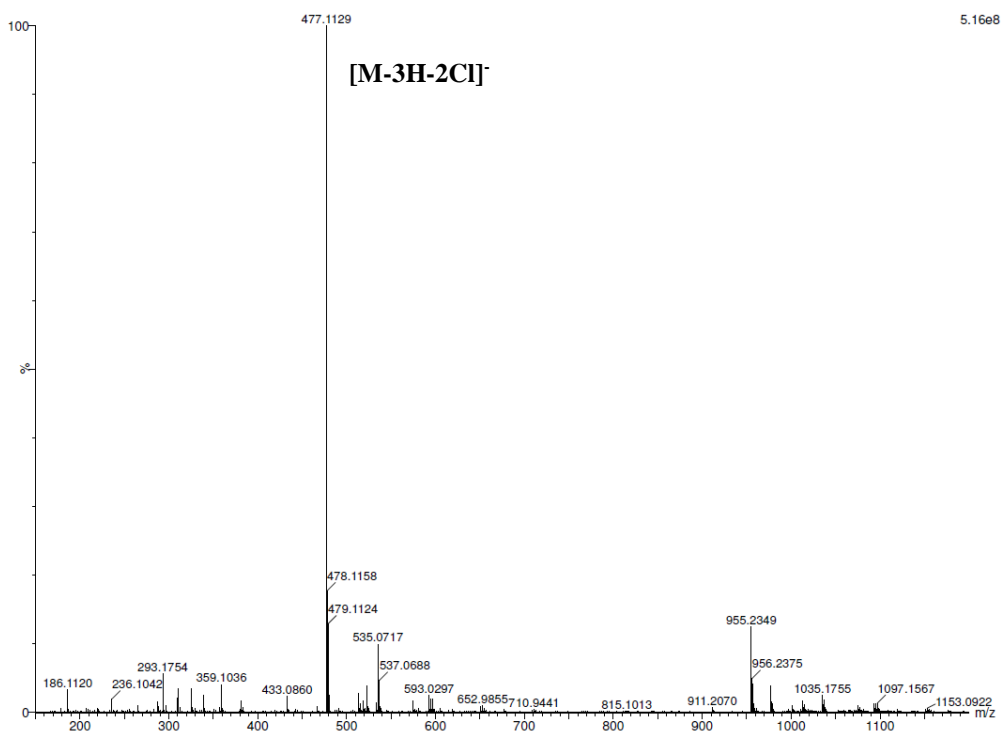


Figure S68. HRMS (ESI) spectrum of 17.

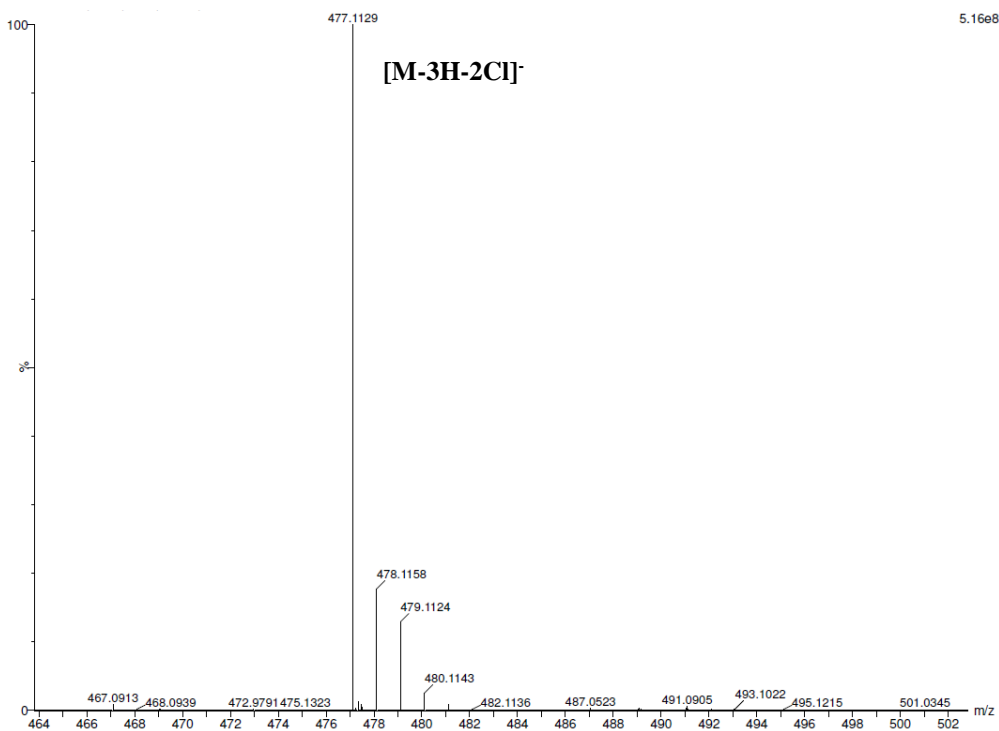


Figure S69. Partial HRMS (ESI) spectrum of 17.

5. Particle size of the PEI-BP-CD ternary conjugates

Table S2. Particle size of the PEI-BP-CD ternary conjugates

Nanoparticle	Size (nm)	SEM
20a	445.9	55.6
20b	450.9	15.8
21a	533.0	45.6
21b	402.8	29.4
22a	529.8	22.1
22b	560.3	27.5

The nanoparticle size was determined using the Zetasizer μ V instrument (Malvern) and 50 μ l UV-transparent Disposable cuvettes (Sarsted). A 0.1 mg/ml suspension of nanoparticles (PEI- β CD or PEI-BP derivatives) was prepared in PBS and the measurement was carried out at 25°C with a refractive index of the sample of 1.53 and A=0, with 3 cycles of 15 measurements of 10 s.

6. Subcellular fractionation of MG-63 cells

Table S3. Subcellular fractionation of MG-63 cells

Fraction	Pyruvate Carboxylase		Histone H3	
	DOX	DOXc21a	DOX	DOXc21a
Lysate	100.00 ± 6.68	100.00 ± 10.31	100.00 ± 16.10	100.80 ± 12.80
Cytosol	31.43 ± 9.54	42.73 ± 1.43	16.04 ± 4.54	11.49 ± 0.28
Nuclei	123.40 ± 6.00	84.81 ± 33.64	109.13 ± 15.51	95.67 ± 5.18
Mitochondria	210.73 ± 21.46	210.94 ± 8.38	9.72 ± 2.90	7.61 ± 3.83

Mitochondria from MG-63 cells treated with DOX or **DOXc21a** for two hours were isolated by a differential centrifugation method. Briefly, cells were washed and scraped with 1.5 ml of sterile ice-cold phosphate-buffered saline (PBS, Sigma-Aldrich, Missouri, USA) and centrifuged 10 min at 800 x g. The pellet was homogenized with a mitochondrial isolation buffer (Tris HCl 50 mM pH 7.5; sucrose 250mM, EDTA 1mM) in a Teflon-glass homogenizer at maximum speed for 10 passes. The cell lysate was centrifuged 10 min at 800 x g to remove cell debris and nuclei and then the supernatant was spun 10 min at 10 000 x g to obtain mitochondria enriched pellet and a cytosolic fraction as supernatant. All procedure was carried out in cold conditions (at 4 °C). Markers for each subcellular fraction were measured by Western-blot using an antibody against Pyruvate Carboxylase as mitochondrial marker and against Histone H3 as nuclear marker. Results are means ± S.E.M. (n=4).

7. Effects of inhibitors of internalization routes on DOX_{21b} uptake

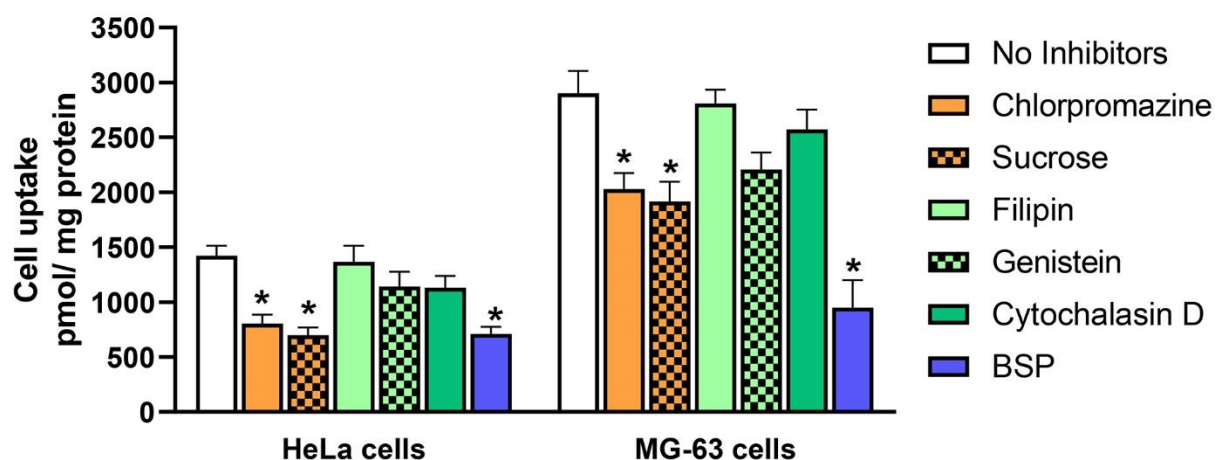


Figure S70. Effects of inhibitors of internalization routes on **DOX_{21b}** uptake. HeLa and MG-63 sarcoma cells were pretreated with chlorpromazine (50 μ M), sucrose (0.45 M), filipin (5 μ g/mL), genistein (400 μ M), cytochalasin D (2 μ M) or bromosulfophthalein (BSP) (0.25 mM) for 30 min before incubation with **DOX_{21b}** (1 μ M). DOX uptake was determined 2 h later. Results are expressed as pmol of DOX/mg protein as means \pm SEM (n = 6). *p < 0.05 vs **DOX_{21b}** treated cells.

8. Specific PEI-BP-CD (20-21b) and PEI-MP-CD (22b) conjugates uptake in bone cells

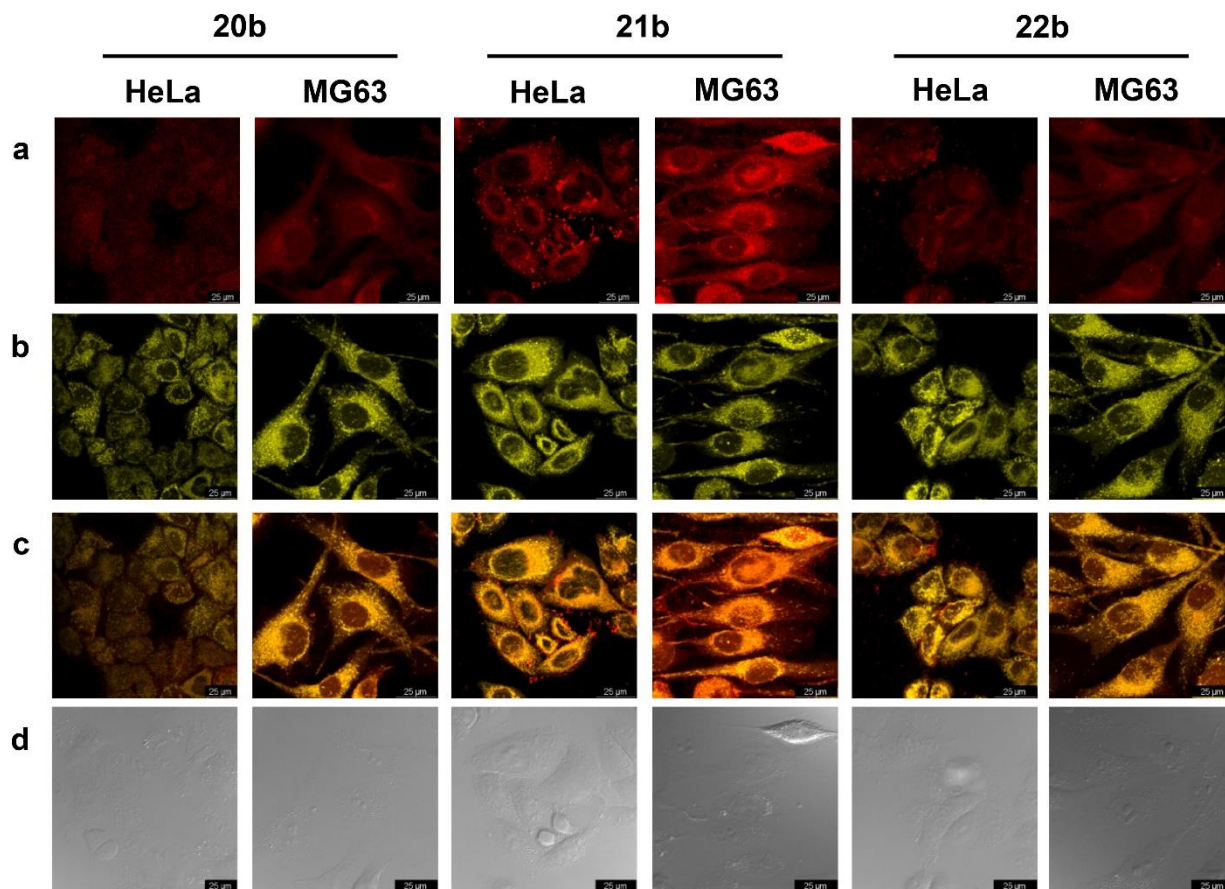


Figure S71. Specific PEI-BP-CD (20-21b) and PEI-MP-CD (22b) conjugates. HeLa and MG-63 sarcoma cells were incubated with mitotracker Deep Red (a) for 30 min, and then with different PEI-BP derivatives containing DOX (b) for 2 hours. Merge (c) and Nomarsky (d) photos are also depicted.

9. *In vivo* imaging of tumor MDA-MB-231 xenografts in mice

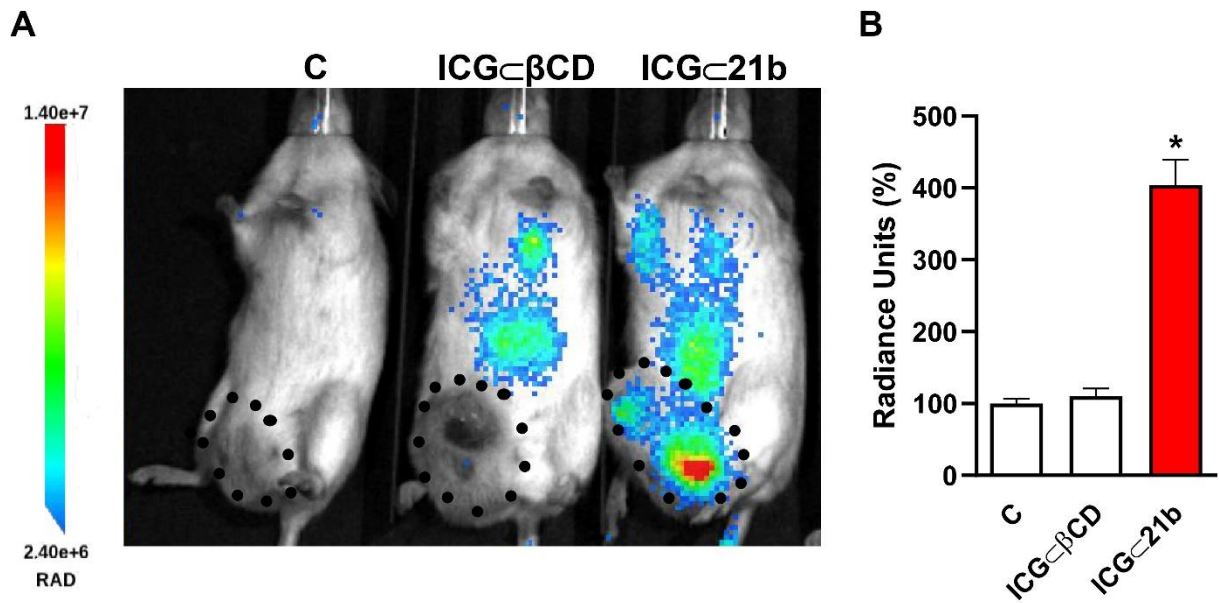


Figure S72. *In vivo* imaging of tumor MDA-MB-231 xenografts in mice. NSG mice bearing breast cancer (MDA-MB-231 cells) tumors were injected intravenously in the tail vein with ICG-βCD or ICG-21b and fluorescence was measured 30 min later. (A) ICG fluorescence images. The size of the xenografts is indicated by a dotted line. (B) Average radiance of the xenografts in vivo. Data are shown as means ± SEM (n = 4). *p < 0.05 vs C animals.